

MAY 2019

M.Sc. in Civil Engineering

FEYZULLAH ÖZEL

**REPUBLIC OF TURKEY
GAZİANTEP UNIVERSITY
GRADUATE SCHOOL OF NATURAL & APPLIED SCIENCES**

**COMPARISON OF MICROTREMOR MEASUREMENTS AND 3-
D SOIL STRUCTURE INTERACTION ANALYSIS FOR A
HISTORICAL MASONRY ARCH BRIDGE UNDER NEAR-
FAULT AND FAR-FAULT EARTHQUAKES**

**M.Sc. THESIS
IN
CIVIL ENGINEERING**

**BY
FEYZULLAH ÖZEL
MAY 2019**

**COMPARISON OF MICROTREMOR MEASUREMENTS AND 3-
D SOIL STRUCTURE INTERACTION ANALYSIS FOR A
HISTORICAL MASONRY ARCH BRIDGE UNDER NEAR-
FAULT AND FAR-FAULT EARTHQUAKES**

**M.Sc. Thesis
in
Civil Engineering
Gaziantep University**

**Supervisor
Assoc. Prof. Dr. Hamza GÜLLÜ**

**by
Fezullah ÖZEL
May 2019**



©2019[Feyzullah ÖZEL]

REPUBLIC OF TURKEY
GAZIANTEP UNIVERSITY
GRADUATE SCHOOL OF NATURAL & APPLIED SCIENCES
CIVIL ENGINEERING DEPARTMENT

Name of the Thesis : Comparison of Microtremor Measurements and 3-D Soil
Structure Interaction Analysis for a Historical Masonry Arch
Bridge Under Near-Fault and Far-Fault Earthquakes

Name of the Student : Feyzullah ÖZEL

Exam Date : 03.05.2019

Approval of the Graduate School of Natural and Applied Sciences

Prof. Dr. A. Necmeddin YAZICI
Director

I certify that this thesis satisfies all the requirements as a thesis for the degree of Master
of Science.

Prof. Dr. Hanifi ÇANAKCI
Head of Department

This is to certify that we have read this thesis and that in our consensus opinion it is
fully adequate, in scope and quality, as a thesis for the degree of Master of Science.

Assoc. Prof. Dr. Hamza GÜLLÜ

Examining Committee Members:

Signature

Prof. Dr. Hanifi ÇANAKCI

.....

Assoc. Prof. Dr. Hamza GÜLLÜ

.....

Asst. Prof. Dr. Hüseyin Çağan KILINÇ

.....

I hereby declare that all information in this document has been obtained and presented in accordance with academic rules and ethical conduct. I also declare that, as required by these rules and conduct, I have fully cited and referenced all material and results that are not original to this work.

Feyzullah ÖZEL

ABSTRACT

COMPARISON OF MICROTREMOR MEASUREMENTS AND 3-D SOIL STRUCTURE INTERACTION ANALYSIS FOR A HISTORICAL MASONRY ARCH BRIDGE UNDER NEAR-FAULT AND FAR-FAULT EARTHQUAKES

ÖZEL, Feyzullah

M.Sc. in Civil Engineering

Supervisor: Assoc. Prof. Dr. Hamza GÜLLÜ

May 2019

80 pages

The aim of this study is to compare the microtremor measurements with 3D soil-structure interaction model of historical masonry arch bridge structure which has an important historical and cultural value in our country that regards to near and far fault ground motions. For this purpose, it is evaluated the comparisons between 3D numerical earthquake model and experimental measurements. The historical Yakacik bridge which is thought to belong to the Ottoman period and masonry stone arch form in the town of Oğuzeli in the province of Gaziantep, is studied. As a source of earthquakes in which SSI interaction is evaluated, near-fault and far-fault ground motions are used. Microtremor measurements are made on the several locations of bridge, in situ natural period and spectral amplifications are determined. Spectral responses (resonance status) obtained by microtremor measurements were found to be potentially promising to support the results obtained from SSI modeling. It is observed that the far-fault motion due to SSI influences results in larger responses than near-fault motion. It is found that the experimentally finding of the possibility of resonance case by microtremor is valuable for the bridge.

Keywords: Microtremor Measurements; Spectral Acceleration; Predominant Period; Near and Far-Fault Earthquakes; Soil-Structure Interaction.

ÖZET

TARİHİ YIĞMA YAPILI BİR KEMER KÖPRÜNÜN YAKIN VE UZAK FAY DEPREMLERİ ETKİSİNDE 3D ZEMİN-YAPI ETKİLEŞİMİ ANALİZİ İLE MİKROTREMOR ÖLÇÜMLERİNİN KARŞILAŞTIRILMASI

ÖZEL, Feyzullah
Yüksek Lisans Tezi, İnşaat Mühendisliği
Danışman: Doç. Dr. Hamza GÜLLÜ

Mayıs 2019

80 sayfa

Bu çalışmanın amacı, ülkemizde yakın ve uzak fay zemin hareketleri etkisinde önemli bir tarihi ve kültürel değeri olan tarihi taş kemer köprü yapısının 3D zemin-yapı etkileşim modeliyle mikrotremor ölçümlerini karşılaştırmaktır. Bu amaçla, 3 boyutlu sayısal deprem modeli ile deneysel ölçümler arasındaki karşılaştırma yapılmıştır. Bu çalışmada Gaziantep ili Oğuzeli ilçesinde bulunan Osmanlı dönemine ait tarihi Yakacık taş kemer köprüsü incelenmiştir. Zemin-yapı etkileşiminin değerlendirilerek deprem kaynağı olarak, yakın ve/veya uzak faylardan oluşan deprem hareketi kullanılmıştır. Mikrotremor ölçümleriyle elde edilen spektral tepkilerin (rezonans durumu) SSI modellemesinden elde edilen sonuçları desteklemek için potansiyel olarak ümit verici olduğu görülmüştür. SSI etkisine göre uzak fay depremlerinin hareketinin yakın fay hareketinden daha büyük tepkilerle sonuçlandığı görülmüştür. Deneysel mikrotremor sonuçlarının rezonans olasılığı açısından köprü için değerli olduğu bulunmuştur.

Anahtar Kelimeler: Mikrotremör Ölçümleri; Spektral Büyütme; Hakim Periyot; Yakın ve Uzak Depremler; Zemin Yapı Etkileşimi.



"Dedicated to my family"

ACKNOWLEDGEMENTS

First praise belongs to Almighty Allah with compassion and mercy, which allows me to complete this thesis. I am ever grateful to Allah, the Creator, and the Guardian, and to whom I owe my very existence.

I would like to express my deep gratitude to my Supervisor: Assoc. Prof. Dr. Hamza Güllü, it would be impossible for me to recommend the research project, to guide and encourage continuous guidance throughout my studies without considering the concept of time, and to complete this work without them.

I would like to thank my parents who have brought me to the present day and have their financial and moral support throughout my education and training life. I would like to give special thanks to my wife, for their help and care during this work.

This study was also partially funded by the Graduate School of Natural and Applied Sciences under grant BAP-2018-MF-YLT-18-20. This financial support is appreciated.

I also would like to thank my friend Murat KARAPEKMEZ for his great support, friendship and help.

Finally, I would like to express my sincere gratitude to all those who helped me in the preparation of the thesis.

TABLE OF CONTENTS

	Page
ABSTRACT	i
ÖZET	ii
ACKNOWLEDGEMENTS	viii
TABLE OF CONTENTS	ix
LIST OF TABLES	xi
LIST OF FIGURES	xii
CHAPTER 1	1
INTRODUCTION	1
1.1. General	1
1.2. The history of the Yakacık bridge	3
1.3. Description of Near and Far-fault Earthquakes	4
1.3.1. Forward Directivity Effect	5
1.4. Description of Soil-Structure-Interaction (SSI)	6
1.5. Description of Microtremor Measurements	7
1.6. Structural Properties of the Bridge	8
1.7. The Significance of Research	8
1.8. Scope of the work	9
1.9. Thesis Organization (Outline of the thesis).....	10
CHAPTER 2	11
LITERATURE REVIEW	11
2.1. Effect of Near and Far-fault Earthquakes on Previous Studies	11
2.2. Effect of SSI on Previous Studies	12
2.3. Microtremor Measurements on Previous Studies	13
2.4. Boundary Conditions.....	14
2.4.1. Elementary Boundary	14
2.4.2. Local Boundary	15
2.4.3. Consistent Boundary	15
2.5. Structural Modeling of Masonry Stone Arch Bridge	15

2.5.1. Micro modeling	16
2.5.2. Simplified micro modeling.....	16
2.5.3. Macro modeling	16
CHAPTER 3	18
METHODOLOGY.....	18
3.1. Selection of Near and Far-fault Earthquakes.....	18
3.2. SSI Methodology.....	21
3.3. Microtremor Measurements	25
3.4. Description of Modeling of Structure (bridge) and Soil	28
CHAPTER 4	39
RESULTS AND DISCUSSION	39
4.1. Influences of SSI Modeling.....	39
4.2. Spectral responses by microtremor measurements	49
4.3. Comparison of microtremor measurements with SSI and fixed base analysis	59
CHAPTER 5	61
CONCLUSION.....	61
5.1. Conclusion.....	61
REFERENCES.....	63
CURRICULUM VITAE.....	80

LIST OF TABLES

	Page
Table 3.1 The near-fault and far-fault earthquake records used in the study [86]. ..	20
Table 3.2 The estimated spring Stiffness of foundation for three different types of soil [97].....	24
Table 3.3 Technical Specifications for SARA SR04S3-10 Accelerometer.	27
Table 3.4 Proposed material properties[46].	30
Table 3.5 Historical development of compression strength of mortar of historical structures [125].....	31
Table 3.6 Compression strength of mortar based on compression strength of stone and mortar group [126].....	31
Table 3.7 Some proposed soil characteristics of bridge's substructure [127].	34
Table 4.1 Comparison of SSI and with fixed base	44
Table 4.2 Spectral responses (spectral amplification, predominant (fundamental) frequency and predominant period) of bridge obtained from microtremor measurements using the estimation methodologies of HVSR (Nakamura's technique), HSR(soil) and HSR(base) [73] (Responses of bridge's base (mt24 base), soil (mts-1, mts-2, mts-3) and bedrock (mt bedrock) are also included for HVSR).....	55

LIST OF FIGURES

	Page
Figure 1.1 Important Roads in Anatolia and historical sites and road connections near the city of Gaziantep and the city in the Ottoman period [2].	2
Figure 1.2 Anatolian Ottoman period roads, 260 bridges and the location of Yakacık bridge [3].	2
Figure 1.3 The top view of new reinforced concrete bridge and historical Yakacık bridge.....	3
Figure 1.4 The north view of Yakacık bridge.	4
Figure 1.5 Directivity effect as forward, reverse, or neutral in the site [9].	6
Figure 2.1 Three types of mesh boundary a) Elementary boundary b) Local boundary c) Consistent boundary [13].	15
Figure 2.2 Numerical masonry model a) Micro b) Simplified micro c) Macro [78, 82].	17
Figure 3.1 A typical comparison of time histories of ground motion velocities [23]: a) near-fault, b) far-fault.	18
Figure 3.2 Active fault map for the region (Gaziantep, Turkey), where the Yakacık bridge is located [83].	19
Figure 3.3 Amplitudes (acceleration, velocity, displacement) versus time plots of earthquakes employed in the study (2017 Kahramanmaraş/Turkey) [86].	21
Figure 3.4 SSI typical view and boundary conditions: a) direct analysis approach [87], b) Boundaries of semi-infinite region (soil) local boundary (viscous dashpot) [13].	23
Figure 3.5 Typical locations of microtremor measurements.....	26
Figure 3.6 Investigated historical bridge in the study:a) General photograph of bridge, and front section views, b) Aerial photograph of bridge and top section views with dimensions of structural parts in west and north (modified from) [110].	33

Figure 3.7	Infrastructure of the bridge: a) Geological map of region [130], b) A typical soil profile of bridge's infrastructure relating to RQD values [127].	36
Figure 3.8	FEM of bridge and infrastructure: (a) FEM for fixed base of bridge (b) FEM for SSI of bridge and infrastructure with viscous dashpot (B= width of bridge, L=length of bridge, 3B =width of infrastructure (soil) boundary, 3 L=length of infrastructure (soil) boundary).....	37
Figure 4.1	SSI influences for the amplitudes (typically at the critical point for the big arch at the inner top): a) fixed base solution, and b) SSI analysis.	40
Figure 4.2	SSI influences for spectral responses of response spectrums (typically at the critical points for the big arch at the inner top, small arch at the inner top and pier at left upper): a) fixed base solution, and b) SSI analysis. i) (S(T)=Spectral acceleration ratio or spectral amplification; ii) Design spectrum in accordance with TSC (2007) [140]; Spectral acceleration ratio (S(T)=normalized spectral acceleration to peak acceleration).	41
Figure 4.3(a)	Fixed base solution.....	42
Figure 4.3(b)	SSI analysis.....	43
Figure 4.4(a)	Horizontal to vertical spectral ratio (HVSR, Nakamura technique). ..	51
Figure 4.4(b)	Horizontal spectral ratio of bridge to soil (HSR(soil), [73].....	52
Figure 4.4(c)	Horizontal spectral ratios of bridge to base of bridge(HSR(base), [73].	53
Figure 4.5	Response spectrums obtained by microtremor measurements for bridge's base, soil and bedrock.	54
Figure 4.6	HVSR versus HSR(soil) and HSR(base) for: a) amplification (S(T), and b) predominant period (Tp) (y=x means perfect fit; mean and standard deviation are estimated from residuals).....	57

- Figure 4.7** Comparisons of spectral amplifications (S(T)) of microtremor measurements (Nakamura method) with SSI and fixed under the effects of a) near-fault b) far-fault earthquakes..... 60
- Figure 4.8** Comparisons of predominant periods of microtremor measurements (Nakamura method) with SSI and fixed under the effects of a) near-fault b) far-fault earthquakes..... 60



LIST OF SYMBOLS

$f_{c,mas}$	Compressive strength of masonry unit
$f_{c,st}$	Compressive strength of stone
$f_{c,mo}$	Compressive strength of morta
$\{\ddot{u}_g(t,x,y,z)\}$	Vector of unknown nodal point displacements
$[M]$	Mass matrix
$[K]^*$	Complex stiffness matrix
$\{u\}$	Vector of unknown nodal point displacements
ν	Poison ratio

LIST OF ABBREVIATIONS

FEM	Finite Element Method
S(T)	Spectral Acceleration Ratio
T_p	Predominant Period
f	Frequency
HVSR	Horizontal to Vertical Ratio
HSR	Horizontals Ratio
SSI	Soil-structure interaction
V_s	Shear wave velocity

CHAPTER 1

INTRODUCTION

1.1 General

The historical structures should be attended in a great importance because of their significant value of cultural heritage that connects past to future to present. The historical structures make an important contribution to the present world about the past civilizations. Anatolia has hosted many civilizations from past to present. The Ottoman Empire was in a significant transition area due to its geographical position. Particularly, the fact that a part of the historical silk and spice road passes through the territory of the country has given the Ottoman Empire a commercial potential and strategic importance. During the Ottomans, there were three main roads in Anatolia that were centered in Istanbul. These roads were called right, left and middle branch (Fig.1.1) [1,2]. Ottomans, caravansarays, hammams, bridges, etc. along these roads, they built a number of structures and provided a suitable environment for the development of trade. One of the historical structures that connect these roads is the historical masonry arch bridges. The masonry arch bridges, which have a historical heritage value from the past to the present, are in the main transportation routes during the period they were constructed. The historical masonry arch bridges in our country, many of which kept until the present day, provide important information about our cultural history. There are 260 masonry bridges from the Ottoman period, between the years 1299-1923 in Turkey (Fig.1.2) [3]. Many of these historic arch bridges have been damaged or destroyed by being exposed to external factors such as war, fire, flood, and earthquake etc. Therefore, if we want to learn more about our past history, it is important to preserve this historical heritage and to transfer on to future generations [4]. It is very important to determine the structural behavior and to know how the method will affect the dynamic properties of the bridge in the repair and restoration of masonry bridges, Today's computer programs with finite element method contribute

to for their preservation efforts and to predict possible responses under the static and dynamic loads [5].

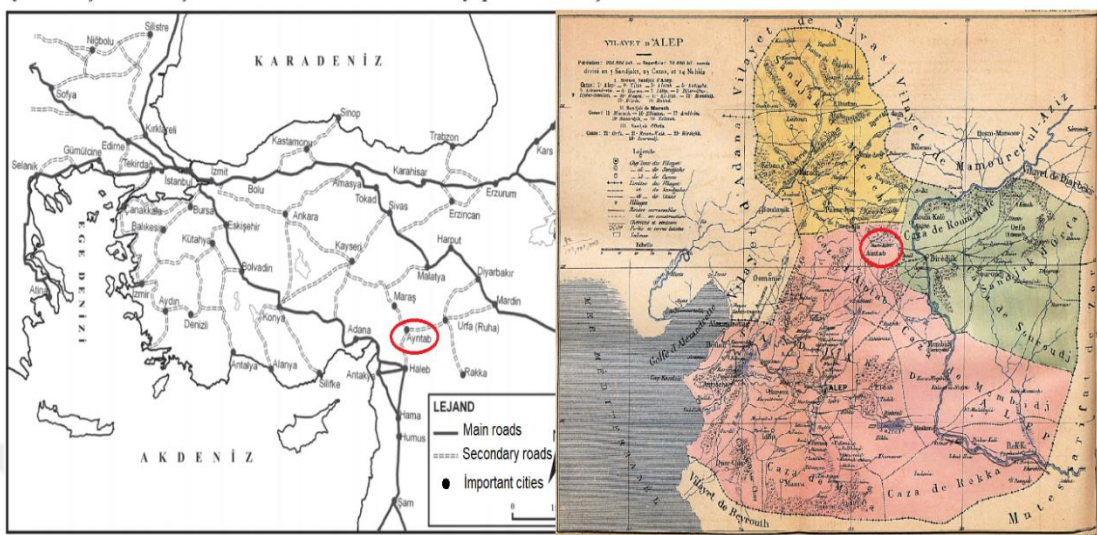


Figure 1.1 Important Roads in Anatolia and historical sites and road connections near the city of Gaziantep and the city in the Ottoman period [2].

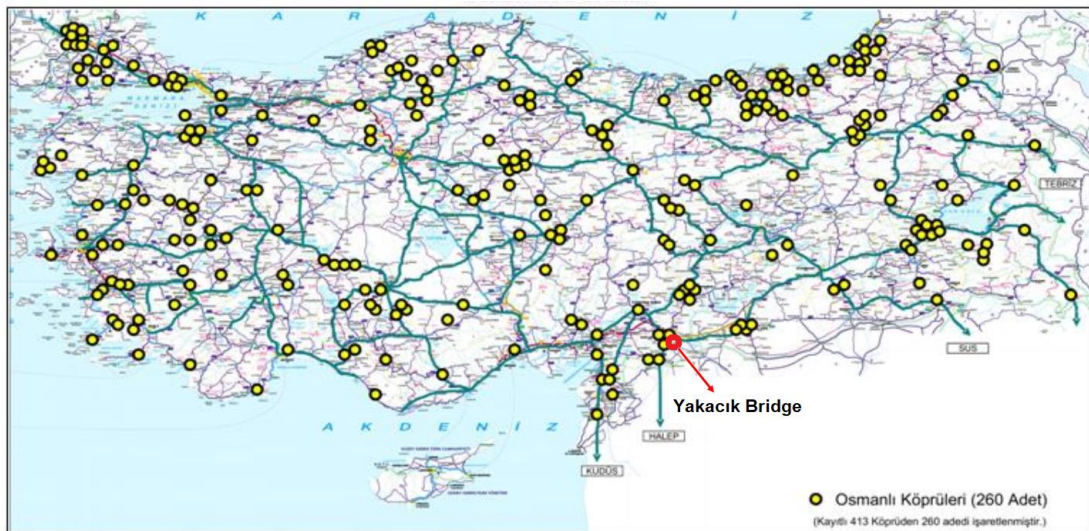


Figure 1.2 Anatolian Ottoman period roads, 260 bridges and the location of Yakacık bridge [3].

1.2 The history of the Yakacık bridge

The structure examined in this research is a historical masonry arch bridge named as Yakacık bridge located in Oğuzeli town of Gaziantep city (Turkey) (Fig.1.3). The bridge is constructed on Sacir stream and located in east-west direction. Yakacık Bridge, between the ancient route of Gaziantep and Tilbasar Castle; it is located on the road that connects the village of Yakacık to Küçük Karacaören village. In the source researches on the historical Yakacık bridge with no inscriptions and information on the bridge was found. It is thought that the bridge should be dated to Ottoman period [6].

The bridge has been repaired in different periods; Finally, in 2005, due to the transition of heavy tonnage vehicles, the south direction has partially collapsed and has become unusable. For this reason, a new reinforced concrete bridge was built on the south side of the historical Yakacık bridge and the traffic flow is provided on this new bridge (Fig.1.3).



Figure 1.3 The top view of new reinforced concrete bridge and historical Yakacık bridge.

The bridge constructed by two arches and one pier has the dimensions of 30m length and 3.80m width. The big (right) arch has the span length of 6m and height of about 4.5m (Fig.1.4).



Figure 1.4 The north view of Yakacık bridge.

1.3 Description of Near and Far-fault Earthquakes

Ground motions occurring near an earthquake fault can be significantly different from those recorded away from seismic sources. The differences between the strong ground motions recorded in the near fault zones and far fault zones are largely due to the earthquake characteristics, including the origin, epicenter distance, local site conditions, and direction from the fracture location [7-9]. Ground motions in the near fault region are significantly affected by the rupture mechanism of the fault, the direction of the fault relative to the region and the permanent displacement of the tectonic movement [10]. The near-fault ground motions (1989 Loma Prieta, 1995 Hyogoken Nanbu, 1994 Northridge, 1999 Chi-Chi) are characterized by a large velocity pulsed ground motion that exposes buildings to high input energy at the beginning of the earthquake. As well as intensive vulnerability of near-fault earthquake observed in past studies [9, 11], the far-fault earthquakes that travel in long periods through long distances could also lead to structural damage specifically for low rise structures dependent upon the velocity spectrum intensity, Housner intensity and spectral acceleration [12] and for medium to high structures due to resonance effect

[13-14]. The earthquake excitation is employed for the strong ground motion from near-fault earthquake (epicenter distance < 10 km) [9, 15-18] and far-fault earthquake (epicenter distance between 10 km-100 km) [12, 17-19] in both.

Earthquake directivity is the focus of wave energy in the direction of rupture along the fault. Orientation of the fault, the direction of slip on the fault, and the location of the recording station relative to the fault affect the ground motion velocity pulses. Therefore this effect is named as directivity effect due to the spreading of the rupture toward the recording site [8, 10, 20-23]. The main characteristics of near-fault ground motions are the effects of the directivity and the fling step leading to serious structural damage in the last major earthquake [24]. The directivity effect could be considered dangerous for resonance reaction due to forward directivity defined as the higher amplitude in shorter duration and backward directivity defined as lower amplitude in longer duration [9, 22].

1.3.1 Forward Directivity Effect

According to the direction of rupture propagation consistent to the site, directivity effect could be categorized into forward, backward and neutral as illustrated in Fig. 1.5 [9]. Neutral directivity effect is occurred at sites which are location off to the side of the fault rupture surface when the rupture propagation is neither predominantly towards nor away from the site. Backward directivity effect occurs in areas near to fault fracture and epicenter give rise to the opposite effect: long duration motions having low amplitudes at long periods [25]. The forward directivity effect in strike-slip faults, the fault direction of the fault towards the region, the center of the earthquake distal, the fault occurs near the surface of the rupture occurs. The forward directivity effect is due to the fact that the rupture speed of the fault is less than the propagation rate of the shear wave. The forward directivity effect occurs in the perpendicular direction to the fault rupture and this increases the potential for damage to ground motions [10, 26]. Forward directivity effects can be consisted both for strike-slip and dip-slip occurrences. When the rupture waves begin to radiate on the fault, forward directivity effect reaches largest velocity in end of the fault in strike-slip events. Forward directivity effects occur for sites in the location where is the up-dip projection of the fault plane [27]. The forward directivity effect is the property of the

near fault ground movements with the highest damage potential. Due to the forward directivity effect, the pulses and large velocity values occurring in the ground motion records are the most basic parameters that determine the engineering characteristics of the near fault ground motions.

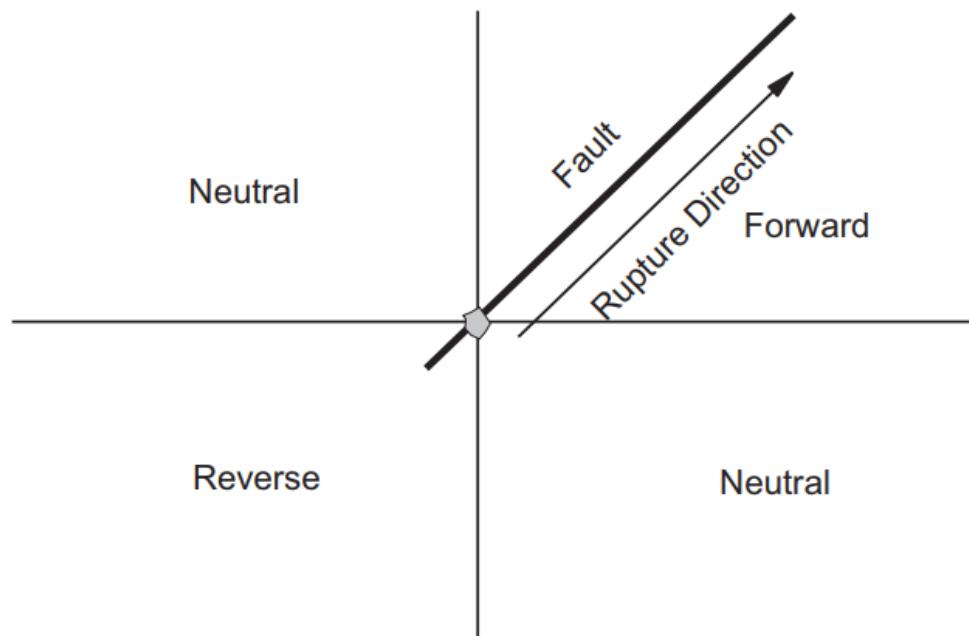


Figure 1.5 Directivity effect as forward, reverse, or neutral in the site [9].

1.4 Description of Soil-Structure-Interaction (SSI)

The response of the soil affecting the structural reaction and the response of the structure affecting the soil reaction under dynamic interactions can be defined as SSI. This means that both ground reactions and structural responses are interdependent under earthquake loads or other dynamic sources affecting structures [13, 28-29]. In clear evidence, structural response is dependent not only on the structural properties but also on the soil properties of structure foundation [30-31].

It is reported [32] that the SSI plays a significant role to increase seismic base shear of low-rise building frames, while seismic response decreases for medium and high-rise

buildings. The effect of the site layering on the resonance of SSI system has been evaluated by some previous efforts [33-34].

The most important factors of the ground motions are earthquake source, propagation effects, local soil conditions with structural features. These factors significantly affect the structural responses, taking into account the SSI effects [35]. It is reported that the acceleration of the structures is significantly affected by the flexibility of the soil and the interactions between the structure and infrastructure soil [36].

1.5 Description of Microtremor Measurements

Microtremor (or ambient vibration) measurement is one of the simplest in-situ testings to identify dynamic modal properties (spectral amplitudes, natural frequencies, etc.) of existing historical structures [37-39]. Based on the seismic noises or ambient vibrations (i.e., wind excitations, sea waves, traffic, machinery, etc.), the microtremor techniques are able to evaluate the mechanical properties of the Earth's subsurface, specifically of seismic velocities [40-41].

Nakamura (1989) relatively popularized the application of the microtremor measurements by offering a simple analysis (the horizontal-to-vertical spectral ratio) for estimating predominant frequency and amplification factor of soil sites [41-44]. It can be said [39] that in cases of historical structures, this computation method using microtremor might be reasonable for frequency estimations particularly when the site amplification is not much strong.

Numerical modeling of historical bridge structures corresponds well to the microtremor measurements for dynamic structural characteristics (such as natural frequencies and modes, vibration measurements of velocities and accelerations) [37] and first three natural frequencies [38]. Masonry buildings have also been assessed using microtremors that offer valuable information and good insights for researchers [45].

1.6 Structural Properties of the Bridge

The building researched in this study is a historical masonry arch bridge named Yakacık bridge which is located in Oğuzeli town of Gaziantep city (Turkey) (Fig 1.3) Despite the limited information (no inscription), it is historically thought to have 200-300 years old back to Ottoman period [6]. The bridge constructed by two arches and one pier has the dimensions of 30m length and 3.80m width. The big (right) arch has the span length of 6m and height of about 4.5m. The detail of dimension can be seen section and plan views (Fig.3.5). The limestone, which is called Gaziantep limestone in Gaziantep city, is the main material of masonry stone structures. The material characteristics (i.e., unit weight, Poisson ratio, compressive strength, tensile strength, modulus of elasticity) of the bridge stone used in this study are proposed (Table 3.4) benefited from previous works [46, 47].

1.7 The Significance of Research

Historical masonry structures like a bridge that includes various structural parts such as arch, pier, etc., it could be important to consider the effect of near and far-fault earthquakes primarily the response of acceleration, velocity, displacement, stress distributions, etc. It could also be important to consider the modeling capability of the bridge by performing microtremor measurements to compare performance for spectral amplitudes and natural frequencies.

Structural responses (ie acceleration, velocity, displacement, spectral acceleration, stress distributions, etc.) depending on masonry structures have also become an important issue under the influence of soil-structure interaction [48-51].

To the authors' knowledge, despite its importance of historical heritage for the region, the historical masonry arch bridge investigated in this study has not been studied up to now for the research interests mentioned above (i.e., comparison of SSI modeling with microtremor measurement). Hence, this paper presents research significance for protection of the investigated bridge with necessary recommendations obtained in this study and transferring well to next generations.

1.8 Scope of the work

This study presents a primary objective for better understanding comparison of microtremor measurements and 3-D SSI regard to the effect of near and far fault ground motions specifically employed for a relatively historical masonry bridge (Gaziantep Yakacık bridge located in Gaziantep city, Turkey).

For this purpose, firstly it is aimed to compare the effects of near and far-fault earthquakes with fixed case of the 3D structural model of historical masonry bridge, for spectral accelerations by response spectrums as well as responses of accelerations, velocity, displacements and stress distributions.

Secondly, using earthquakes (1 near-fault, 1 far-fault are selectede and scaled to the peak ground accelerations) determined from the comparison, a 3D dynamic soil-structure interaction (SSI) analysis has been performed for a further comparison of the near and far-fault effects on responses of the historical masonry bridge. All earthquake responses were obtained using the loading condition of time-history analysis taking linear behavior into account. Using solid elements, the structural model of the masonry bridge in 3D was built with finite element method (FEM).

Thirdly, spectral amplification, predominant period and local soil, base of structure and bedrock behavior were searched by means of microtremor measurements on the historical bridge. Two methodologies primarily were used: i) H/V ratios (the horizontal-to-vertical spectral ratio) using the method of Nakamura [71] that can be notated by HVSR, and ii) the ratio of horizontal spectral component of structure to horizontal spectral component of soil or free-field recommended by Gosar [73].

Then for understanding the capability (suitability) of bridge modeling, microtremor measurements (using Nakamura technique) were compared with SSI analysis and fixed base model under the effects of near and far-fault earthquakes. To the author's knowledge, for the historical masonry bridge researched in this paper, the research issues considered above (i.e., near and far fault effects, SSI influences, comparing the results of microtremor measurement and FEM modeling) have not been sufficiently studied, despite of its importance historical heritage.

Therefore, the effort presented here provides some important explanations for the safety and preservation of the existing historical bridge and for the future generations well. Since many such historical masonry bridges exist in the country (Turkey), this study could also contribute to other masonry bridges being seismically concerned.

1.9 Thesis Organization (Outline of the thesis)

This thesis contains of five chapters.

Chapter 2 presents a review of the literature of previous studies on near and far-fault earthquakes, SSI, Microtremor include general informations about boundary conditions and structural modeling.

Chapter 3 Define methodology of selection earthquakes (near and far-fault), SSI methodology , Microtremor measurements and describing bridge throughout study.

Chapter 4 Provides the results of the study. Moreover, how the consideration of near and far-fault motions including SSI effects on amplitudes (acceleration, velovcity, displacement), response spectrums and stress distrubutions, microtremor measurements, comparing spectral acceleration and periods using HVSR and HSR. List of results, Figures, evaluation are illustrated and discussed.

Chapter 5 gives conclusions of the thesis.

CHAPTER 2

LITERATURE REVIEW

2.1 Effect of Near and Far-fault Earthquakes on Previous Studies

The effects of near-fault and far-fault ground motions on civil engineering structures have been investigated in many recent studies [9-10, 12, 14-15, 17, 19, 22-23, 27, 52-55].

It was compared with some aspects of the response of the elastic and non-elastic SDF (single degree freedom) systems to the ground motions of the near and far fault [14], and it was reported that near-fault ground motions impose a larger strength demand than far-fault motions for same ductility factor.

The characterization of the forward directivity pulse motion of near-fault earthquakes has been described in a previous study of key parameters including amplitude (peak ground velocity), velocity pulse period and significant number cycles [10, 22].

Responses of near-fault forward directivity ground motions were studied and It was found that site effects should be accounted for when designing structures to resist near-fault forward directivity motions and the nonlinear effects of local site conditions should be addressed in near-fault regions when considering forward directivity motions [53].

It was compared the effects of near and far-fault ground motions on geometrically nonlinear earthquake behavior of suspended bridges [15] and it was found that the maximum displacements from suspension bridges obtained for near-fault ground motion and maximum internal forces are more effective than those for far-fault ground motion.

The effects of ground motion near and far fault ground motions on non-linear dynamic response were presented the results of a study aiming to evaluate the seismic damage of concrete gravity dams including dam reservoir foundation interaction and It was reported that near fault ground motions have the potential to cause more serious damage than far fault ground motions in the dam body. [9]

The degree of correlation was investigated between the various seismic parameters of the far fault ground motions and the structural damage under the earthquake in low-rise reinforced concrete structures by using nonlinear time history analyses in recent study [12] and it was found that the velocity spectrum intensity is the best identifier of the seismic damage potential of far fault ground motions.

It was investigated that the seismic performance of old concrete bridges with different column heights on near and far fault sources were evaluated by seismic fragility curves. The fragility curves can be used to assess potential losses of bridges with the same typology of the analyzed structure. The results showed that the seismic records in the far fields were dominant and the effect of the earthquake databases in the near fields decreased [17].

2.2 Effect of SSI on Previous Studies

Despite a significant effort in previous works, it is well known that the dynamic response of the historical masonry bridges is governed by the surrounding soil, and a soil-structure interaction (SSI) analysis regarding the effect of soil by a realistic model is neglected in most of them. Furthermore, no effort of SSI modeling compared with experimental results appears specifically for understanding the model ability and seismic performances.

Soil-structure interaction (SSI) clearly plays a primary role on the dynamic performance of structures against earthquake effects observed in many past earthquakes such as 1985 Mexico City, 1989 Loma-Prieta, 1992 Erzincan, 1995 Kobe, 1995 Dinar, 1999 Kocaeli, etc [15-16, 23, 36, 55-59]. It can be defined as both the response of soil affecting the structural response and the response of structure affecting

the soil response under dynamic interactions. This means that neither the ground responses nor the structural responses are independent of each other under the earthquake loadings or other dynamic sources that affect the structures [13, 28].

Regarding many responses, SSI effects have been extensively studied for dynamic issues in the structures observed in past works. It is interesting that the effect of SSI could be of major concern on the dynamic characteristics for low-rise buildings [32]. It is reported [32] that the SSI plays a significant role to increase seismic base shear of low-rise building frames, while seismic response decreases for medium and high-rise buildings.

Some studies propose equilibrium equations for the SSI effect on the frequency and damping for a multi-degree-of freedom oscillator supported by a rigid foundation [60-61]. A concrete gravity dam is investigated for SSI effects by attaching dashpot to vertical boundaries and modeling dam and foundation as linear and elastic materials [62]. Influences of various factors on SSI are studied for seismic response of cantilever walls using 3D modeling [63].

2.3 Microtremor Measurements on Previous Studies

Many past studies have been investigated on measuring ambient vibrations in literature. [38, 44, 64-70]. In recent years the single-station microtremor method has been widely used [43-44, 71-72] on measuring ambient vibrations.

It was emphasised [39] that in cases of historical structures, computational method using microtremor might be reasonable for frequency estimations particularly when the site amplification was not much strong. On the other hand, spectral ratio of horizontal component of acquired microtremor data of structure to ground or free-field was alternately proposed for determining predominant (natural) of structure [73].

The historical bell tower 74 m length which was constructed in the 17th century was studied regard to the environmental vibration tests. The measurement of the structural response to ambient vibration levels has proven to be an effective mean for defining

the dynamic properties of masonry structures, but in some measurements it has been found that the signal to noise ratio is very low. [74].

Determining the modal parameters on the historical masonry palace between the years 1861-1865 in İstanbul experimentally and analytically in previous years studied and the results obtained good consistency between experimental and numerical analysis revealed the dynamic characteristics of the palace [75].

The ambient vibration testing and damage assessment in previous studies [76] were conducted in a historical monastery in England. The results of the vibration tests showed that the vibration tests were successful and fast in determining the wall, dome and vault damages.

The ambient vibration test was investigated in a recent study of the finite element model update and near and far fault ground motion analysis. While analytical and experimentally defined mode shapes exhibited visual agreement, an average of 10% deviation was observed between natural frequencies [38].

2.4 Boundary Conditions

The problems of dynamic response and soil structure interaction are located at a considerable distance from the rigid or near rigid boundaries, especially in the horizontal direction. As a result, the wave energy moving away from the region of interest can be permanently removed from this region. In a dynamic finite element analysis, it is important to simulate such radiation damping behavior. The common boundary types for finite element analyses can be classified into three groups respectively elementary, local and consistent boundaries (Fig 2.1) [13, 28, 77]. In this study, only local boundary (viscous dashpot) is used for SSI analysis.

2.4.1 Elementary Boundary

Zero displacement or zero stress conditions are identified in the basic limits. However, for lateral or lower boundaries, the perfect reflection properties of the elementary

boundaries can catch hold of energy that would propagate past the boundaries and away from the region. This term, expressed as a “box effect”, can produce serious errors in the analysis of a soil response or soil-structure interaction (Fig 2.1a).

2.4.2 Local Boundary

Common local boundary type is termed simply viscous or dashpot boundary which capable of flexibility and energy absorption of body waves but not in surface waves. Since waves are likely to reach the boundary at different angles, a local boundary with a specific indicator point coefficient will always reflect some event wave energy. As a result, the effects of reflections from local boundaries can be reduced by increasing the enough distance between the border and the region of interest (Fig 2.1b).

2.4.3 Consistent Boundary

Consistent boundaries are defined as absorb all types of body waves and surface waves at all angles of incident and all frequencies. The consistent boundary can be employed for all soil structure analysis events (Fig 2.1c).

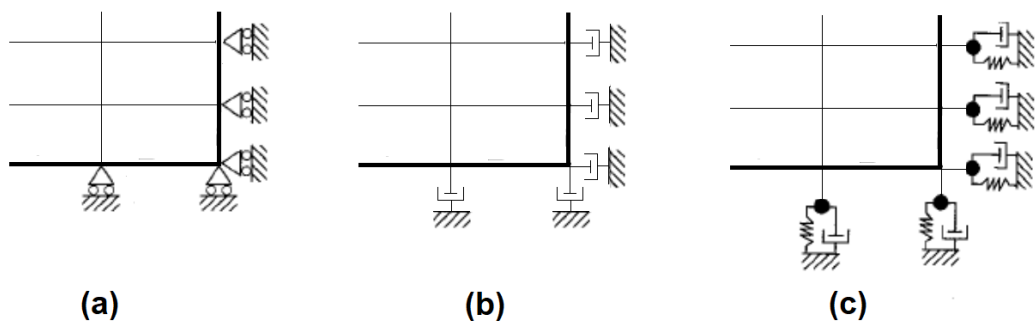


Figure 2.1 Three types of mesh boundary a) Elementary boundary b) Local boundary c) Consistent boundary [13].

2.5 Structural Modeling of Masonry Stone Arch Bridge

One of the most complex problems in structural engineering research and application is numerical modeling of masonry structures which can be known as one of the oldest

building materials that is composed of masonry units (i.e. brick, blocks) with or without mortar. This complexity, size and anisotropy of bricks, joint dimension and positioning of bed and head joints, material characteristics of both brick and mortar and workmanship quality can be connected to many important factors in finite element method. For the numerical modeling of the masonry, micro, simplified micro and macro modelling are used (Fig 2.2) [78].

2.5.1 Micro modeling

Micro modeling of the masonry, where stone/brick, mortar and interface elements are modeled separately (Fig 2.2a). The mechanical properties of each of the materials (brick unit and mortar) which constitute the masonry structure, namely, the Elasticity Modules, Poisson ratios and non-elastic properties are considered. According to the strategy of this method, units and mortars in joints are represented by continuous elements, while unit mortar interfaces are represented by discontinuous elements. While this modeling leads to more accurate results, because of the relevant analysis is computationally intensive and limits the implementation of small scale laboratory samples and structural details. Simplified micro modeling procedures for the solution of this problem have been proposed in previous studies [79].

2.5.2 Simplified micro modeling

Simplified micro modeling is expressed by extending the dimension of stone/brick to half the thickness of the mortar. It has been accepted that cracks that may occur in the masonry may occur at the average interfacial line. The mortar joint is also modeled as a zero-thickness interface. Interface elements are used in mortared stone/brick units which were defined in the finite element mesh (Fig 2.2b).

2.5.3 Macro modeling

Masonry unit and mortar properties are considered as composite material by homogenizing in macro modeling method (Fig 2.2c). The mechanical properties of this model are the values obtained as a result of homogenization process. This model is used effectively for macro modeling of the masonry structures. Through structural

modeling of masonry bridge in this study, a macro modeling, where the masonry structure is considered as an isotropic and homogeneous was assumed conforming to previous studies [80, 81]. In other words, masonry blocks and mortar were simulated with together (i.e., no clearance between masonry blocks and mortar). It has been reported [81] that especially for bridge structures investigated in this study, macro modeling may be thought for simpler solutions.

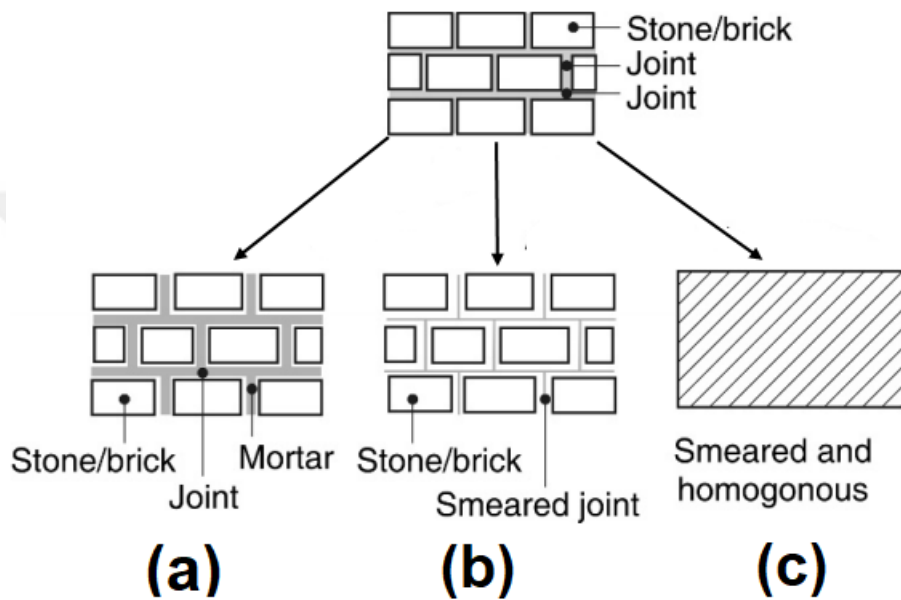


Figure 2.2 Numerical masonry model a) Micro b) Simplified micro c) Macro [78, 82].

CHAPTER 3

METHODOLOGY

3.1 Selection of Near and Far-fault Earthquakes

In this research, the near-fault earthquake affecting the investigated bridge is defined for the strong ground motion record: i) obtained in the vicinity of a fault with apparent velocity pulse (i.e., pulse duration larger than 1.0s) [23], ii) epicenter distance less than 10km, as applied in previous studies [9, 15-18].

Far-fault strong ground motion is selected on contrary to the criterion of near-fault above (i.e., pulse duration less than 1.0s, epicenter distance greater than 10km,) [12,17-19]. A typical comparison of near and far-fault earthquake records in the velocity-time history is shown in Fig 3.1 [23].

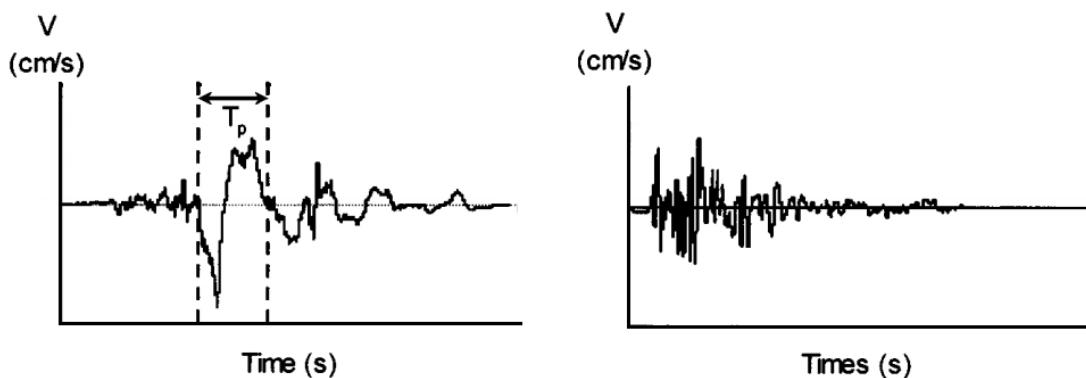


Figure 3.1 A typical comparison of time histories of ground motion velocities [23]:
a) near-fault, b) far-fault.

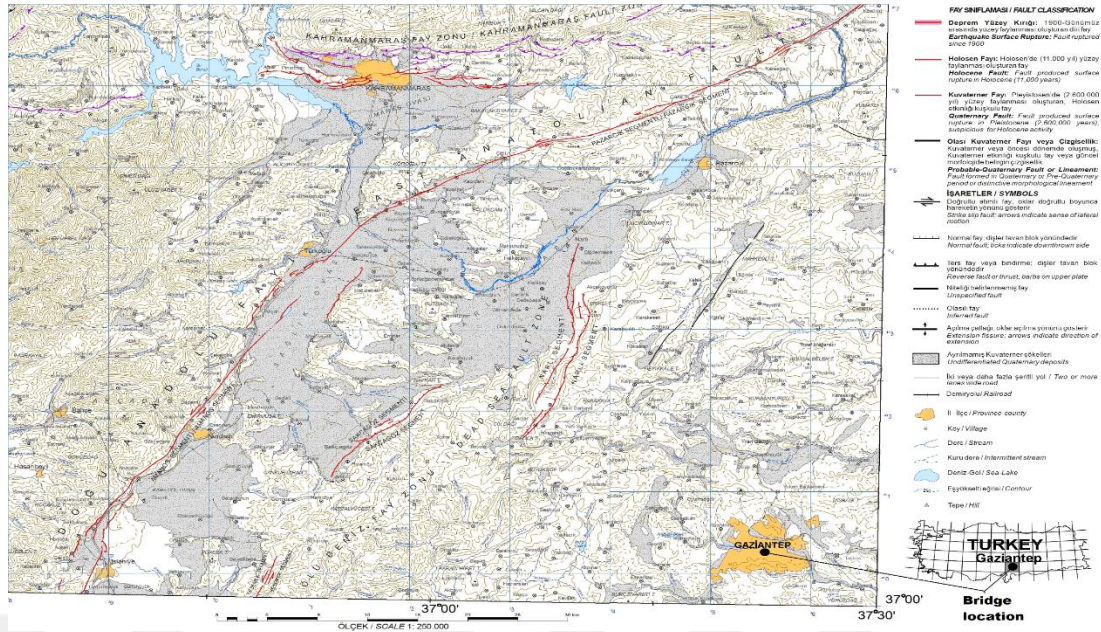


Figure 3.2 Active fault map for the region (Gaziantep, Turkey), where the Yakacık bridge is located [83].

During the selection of earthquakes based on the criteria given above, the earthquake (tectonic setting) of the region (Gaziantep, Turkey) is also taken into consideration. Thus, the earthquakes specifically with the strike-slip type of fault that represent the tectonic mechanism of the region (Gaziantep) due to East Anatolian Fault is used for the investigated bridge (Fig.3.2) [83]. It is reported [84] that the East Anatolian fault appears a relatively earthquake potential expected for the region in near future. Moreover, selected original earthquake records (1 near-fault, 1 far-fault) are scaled to the peak ground accelerations between 0.2g and 0.3g in order for representing the earthquake potential of the investigated region (Gaziantep) [85]. The earthquakes employed in the study are presented in Table 3.1 [86]. The amplitudes (acceleration, velocity and displacement) versus time plots of the earthquakes are also illustrated in Fig.3.3.

Table 3.1 The near-fault and far-fault earthquake records used in the study [86].

Fault for strong ground motion	Earthquake name	Station&Code	Scale Factor	Arias Intensity (m/s)	Vs30 (m/s)	PGA (g)	PGV (cm/s)	PGV/PGA (s)	Mw	Distance to fault Rjb (km)
Near-Fault	2017 Kahramanmaraş (Turkey)	STATOIN ID: 4616	13.00	0.22	390	0.25g	10.26	0.04	4.0	9.87
Far-Fault	2017 Kahramanmaraş (Turkey)	STATOIN ID: 4629	2,115	1.4	-	0.25g	8.97	0.04	3.7	153.20

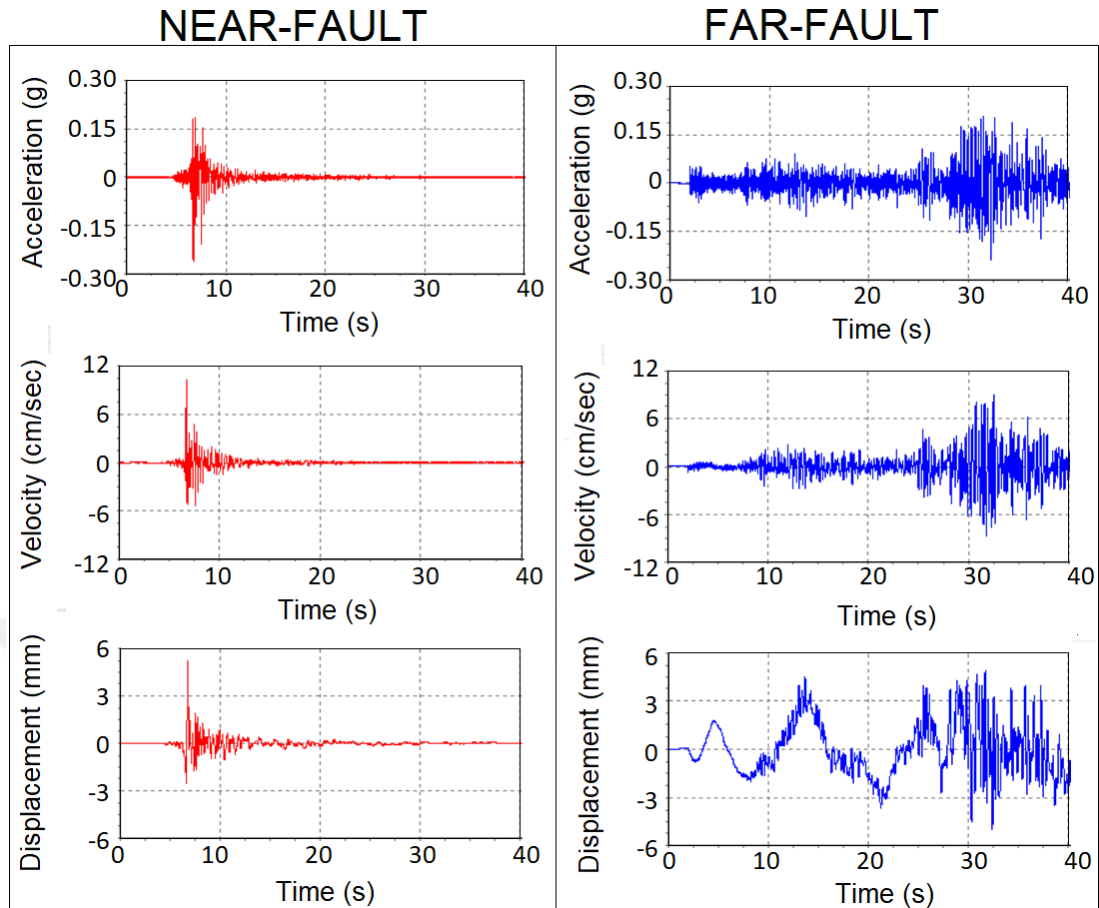


Figure 3.3 Amplitudes (acceleration, velocity, displacement) versus time plots of earthquakes employed in the study (2017 Kahramanmaraş/Turkey) [86].

3.2 SSI Methodology

SSI methodology applied in this work for the earthquake effects on the masonry bridge utilized the direct analysis approach, as typically sampled in a general schematic view in Fig.3.4a [87]. In the direct approach, the soil region near the structure along with the structure is modeled directly and the idealized soil–structure system was analyzed all together as a complete system [62, 87]. Some difficulties of applications of the direct approach (i.e., for 3D nonlinear dynamic analysis and satisfying the radiation condition of the wave field towards infinity) due to excessive storage requirements and computation time, especially for complex structures are reported by past studies [62, 87-88]. However, the direct method is more competent to solve problems in variable loading situations and complex geometries in a single step especially for constructing the SSI system by a finite element model in order to address a elaborate response to structure and soil when exposed to earthquakes [89].

For free field input movements indicated along the base and sides of an SSI model, as shown in Fig 3.4, the resulting response of the interacting system owing to the direct method can be calculated from the equations of motion, as given (Eq. 3.1):

(3.1)

$$[M]\{\ddot{u}\} + [K^*]\{u\} = -[M]\{\ddot{u}_g(t, x, y, z)\}$$

where $\{\ddot{u}_g(t, x, y, z)\}$ is the specified free-field accelerations at the boundary nodal points, $[M]$ is the mass matrix, $[K^*]$ is the complex stiffness matrix, and $\{u\}$ is the vector of unknown nodal point displacements. In this study, the finite element method (FEM) as shown in Fig.3.4b [13] used in the modeling of the near field (soil body) with the direct method application between the soil and the structure was used while the far field (around the soil body) was used by adding some special artificial boundaries, based on the suggestions of past studies [63, 90-92].

The finite element method for the dynamic analysis of the soil body integrates the discrete elements described by the nodal points with the proposition, that the body can be identified by the response of the nodal points of the response [93].

Instead of modeling very large soil volumes for computational adequacy, it is desirable to limit the number of elements (ie, the number of solids or nodes) to a reasonable size. Therefore, finite element analysis of dynamic soil-structure interaction problems, artificial boundaries (transmitting boundaries) should be sufficiently added from the region of interest. This not only avoids unrealistic wave reflections, but also allows the evaluation of the radiation effects to obtain uncomplicated results [28, 63].

The effect of SSI, finite element analysis is studied artificially as the most commonly used artificial boundaries of the semi-infinite region (soil) for the local boundary reported by past work as shown in Fig 3.4b, [13] as earthquake absorbent boundary using a viscous dashpot.

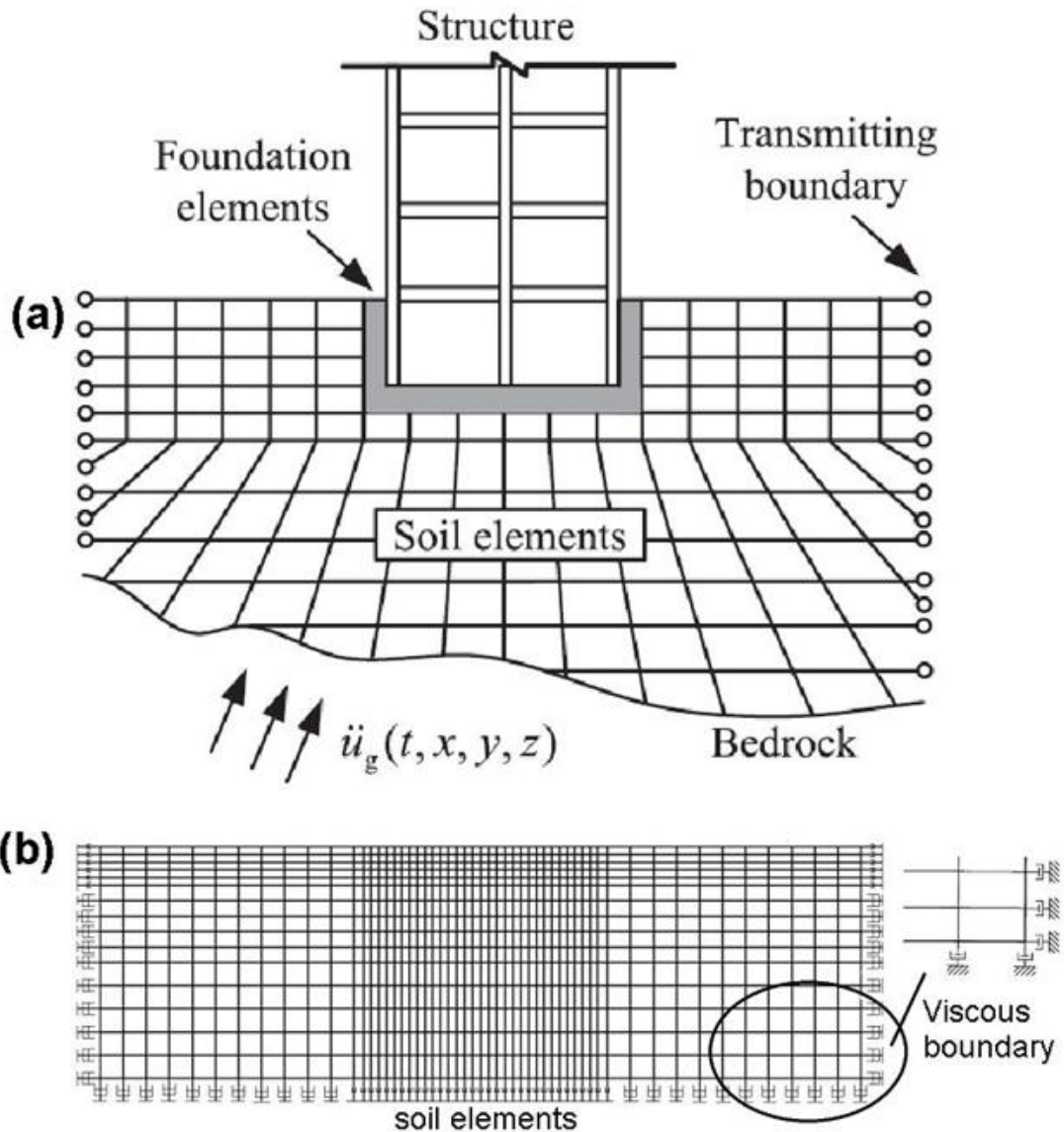


Figure 3.4 SSI typical view and boundary conditions: a) direct analysis approach [87], b) Boundaries of semi-infinite region (soil) local boundary (viscous dashpot) [13].

It has been reported [63] that the viscous boundaries must absorb the energy reflected through the artificial boundaries and this has the advantage of being used independently of the stresses that provide satisfactory responses to body waves. For this purpose, the well-known equation of motion, including the damping matrix (see in detail) is taken into account when calculating the viscous dashpot. On the other hand, when the basic boundary is placed at a sufficient distance between the structure and the soil, it is easier to absorb reflected waves more easily [13]. The viscous boundaries in this study could be of significance for reflecting the distance effect and dynamic responses for future studies. The SSI effect was important in past studies

using the artificial boundary of the viscous dashpot [63, 90]. It is seen from the literature surveying that the SSI effect of viscous dashpot boundaries has a lack of effort.

In this study, to account for soil effects within the SAP2000 (v.20) [98] model, spring supports are defined. The foundations and the members of structure are modeled with statically equivalent springs by considering the foundation and soil structure interaction. As for the modeling the base of structure and soil for SSI analysis, the elastically spring supports having statically equivalent springs are adequately employed in this present study from the proposed stiffness values of spring support for different soils in a past work [97] (Table 3.2). As well as the geological setting and ground characteristics (Table 3.7), the inclusions of clayey and chalky compounds in limestone with weak characteristics of Gaziantep formation [94] become dominant for selection of stiffness values during SSI. Two orthogonal springs, one vertical spring and three rotational springs are defined in the main direction to simulate the SSI effect by the spring supports. A variety of efforts used the similar approach of spring constant are also available in earlier works [95-97].

Table 3.2 The estimated spring Stiffness of foundation for three different types of soil [97].

Direction	Unit	Soft Soil	Medium Soil	Hard Soil
Vertical, Kz	kN/m	8679.07	45897.75	644502.27
Horizontal, Kx	kN/m	5786.05	36936.76	580052.04
Horizontal, Ky	kN/m	5786.05	36936.76	580052.04
Rocking,	kNm/Rad	1472678.00	7787,998.16	109360086.95
Rocking,	kNm/Rad	425510.46	2250,237.11	31598123.26
Twisting,	kNm/Rad	998328.62	6863330.52	111202826.79

Comparisons of near and far fault earthquakes as fixed case and SSI consideration in both have been carried out using time history analysis with linear behavior in this study. FEM software package of SAP2000 (v.20.[98] have been used in 3D modeling

for computations. Previous studies have reported that the SAP2000 program is the software that can solve the dynamic SSI problems correctly [81, 91, 99-100].

3.3 Microtremor Measurements

Among the microtremor methods, the single-station method, which provides practical and faster results, is widely used in recent years [43-44, 71-72]. In this study, experimental dynamic researches on the bridge investigated were conducted only by passive research using ambient vibration tests. In general, use of contact sensors such as seismometers or accelerometers offer many advantages in terms of reliability of results [101]. In order to collect the vibration data in the measurements, the seismic accelerometers were used to collect the signals received from the accelerometers, and the data collection unit and the signal processing programs were used to process the signals. The selection of the accelerometers is very important as it is designed for a specific sensitivity and frequency range [102].

Spectral amplification, predominant period and local soil, base of structure and bedrock behavior were searched by means of microtremor measurements in this study (Fig.3.5). For this purpose, a three-component SR04S3 velocity recorder was used to collect microtremor measurement datas. The technical specifications of used accelerometers were presented in Table 3.3 The choice of test time and sampling rates to ensure appropriate signal quality is important in the ambient vibration test [38].

Microtremor Measurement Points

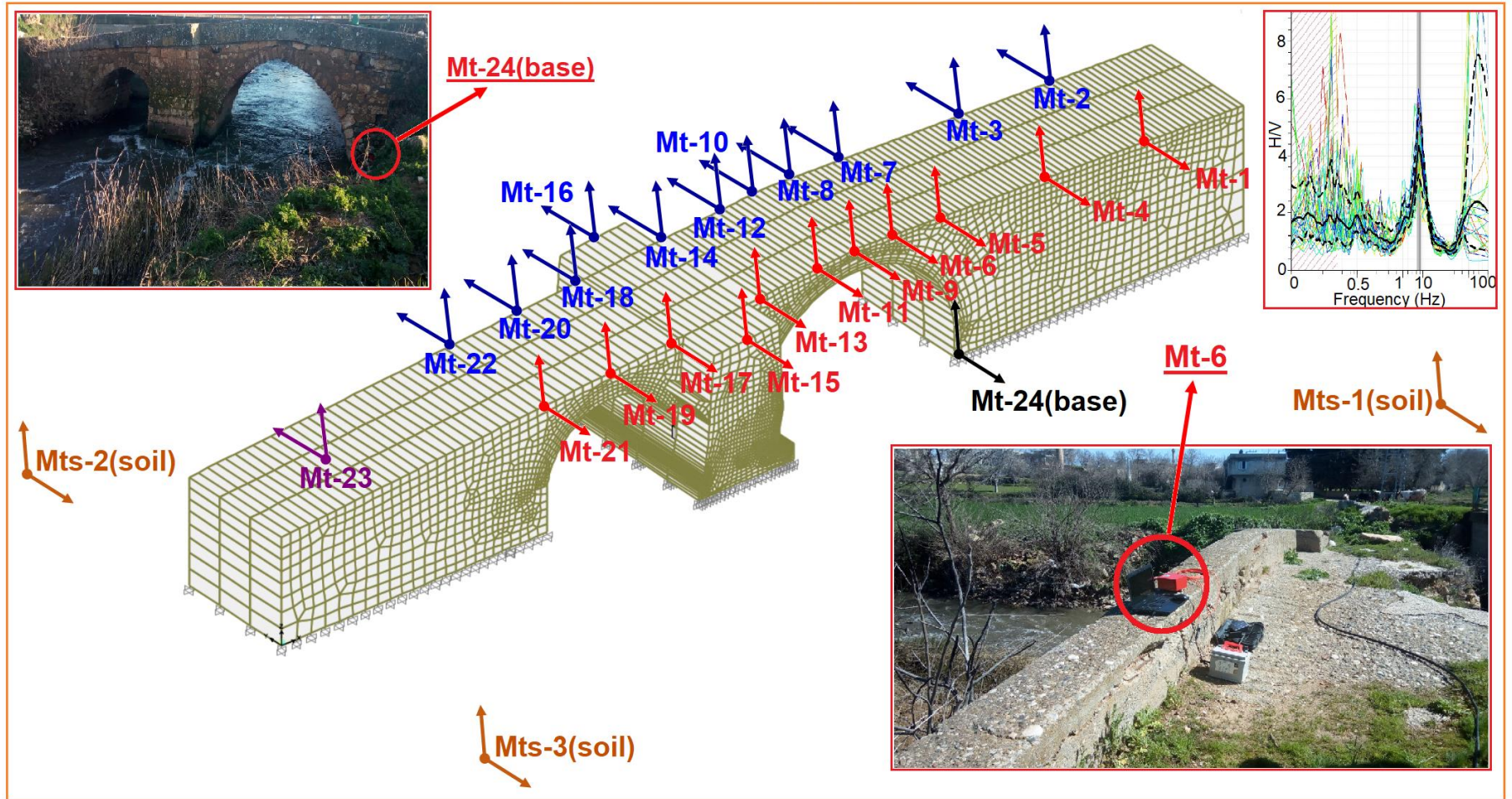


Figure 3.5 Typical locations of microtremor measurements.

Table 3.3 Technical Specifications for SARA SR04S3-10 Accelerometer.

Accelerometer	SARA SR04S3-10		
Numbers of channels	3,24 bit	Operating Temperature	-20/+50°C
Linear Frequency range	1-100 Hz	Dimensions	205x170x45 mm
Communication speed:	115200 baud	Total Mass	<4 Kg

Varying durations were used in the measurement of ambient vibrations in the previous literatures [38, 44, 64-70]. Short-periods sensors are three component seismometers that cover higher frequency bands usually 1 Hz to 100 Hz [103]. Ambient vibration tests of the bridge in 15 min intervals with a selected sampling ratio of 100 Hz. were used in this study. The measurement interval was approximately variable between 30 microtremor points (Fig.3.5) while the recording time was 15 min sampled at 100 Hz. Reducing the effects of environmental and anthropogenic effects such as wind and traffic noise were taken into account during the measurements. In measurements and data evaluation, SESAME project [104] criteria were taken as the basis and the obtained field data were evaluated by using a software [105] that is compatible with the seismometer [106].

The aim is to ensure that the ambient vibrations are constant and to avoid temporary events connected with specific urban resources (footsteps, traffic). After avoiding transients, bigger than ten windows were included for evaluation. For every selected time window, the Fourier amplitude spectra were smoothed with a [107] filter by using a coefficient of 40 for the bandwidth. The final Horizontal to vertical spectral ratio and the associated standard deviation were obtained by averaging the H/V ratios from all windows. One of the H/V spectral ratio versus frequency graph is seen in Figure 3.5

As a consequence of microtremor measurements, spectral amplifications and predominant frequencies of bridge in this work are estimated by two methodologies primarily: i) H/V ratios (the horizontal-to-vertical spectral ratio) using the method of Nakamura (1989) that can be notated by HVSR, and ii) the ratio of horizontal spectral component of structure to horizontal spectral component of soil or free-field recommended by Gosar et al. (2010) that can be represented by horizontal spectral ratios of bridge to soil as HSR(soil). Moreover, the ratio of horizontal spectral amplitudes obtained at the bridge surface to horizontal spectral amplitude obtained at

the base of bridge that can be represented by HSR(base) is computed for spectral amplifications and fundamental (predominant) frequencies of the bridge, again based on the study of Gosar et al. (2010). In all estimations, the frequency that reaches maximal value is taken fundamental frequency.

While the estimations by the ratio of horizontal spectral amplitudes [73] are limitedly known, the horizontal-to vertical-spectral-ratio (HVSr) technique or Nakamura's technique [71], the author that originally proposed the method, gives good estimates of resonance frequency of buildings and soils [72]. Thus, it is expected that the conducted microtremor measurements essentially alongside the surface of bridge could be beneficial for obtaining good estimations of main natural frequency of the bridge. This is also valid for the soil at nearby bridge or free field sites. Determination of fundamental frequencies of a structure and of its soil by microtremor measurements could be capable of determination of the resonance phenomena for promising the structure stability during an earthquake without having any complexity. Regarding the importance of resonance investigated in previous studies [108-109], the experimental effort by microtremors will be also useful for understanding suitability of the modeling of SSI system by linear elastic behavior employed in this study.

3.4 Description of Modeling of Structure (bridge) and Soil

The structure examined in this research is a historical masonry arch bridge named as Yakacık bridge which is located in Oğuzeli town of Gaziantep city (Turkey) (Fig 1.3) Despite the limited information (no inscription), it is historically thought to have 200-300 years old back to Ottoman period [6]. The bridge constructed by two arches and one pier has the dimensions of 30m length and 3.8m width. The big (right) arch has the span length of 6m and height of about 4.5m and the small (left) arch has 4m span width and 3 m height. The height of Pier is 3.5 m. The detail of dimension can be seen section and plan views (Fig.3.6).

The bridge project with the plan dimensions and detailed views (Figure 3.6) was partly provided by the local authorities, and the aerial photo of the bridge was photographed on site [110]. The limestone, which is called Gaziantep limestone in Gaziantep city, is the main material of masonry stone structures. The proposed material properties (i.e.,

unit weight, Poisson ratio, compressive strength, tensile strength, modulus of elasticity) of the bridge stone used in this study are shown in Table 3.4 benefited from previous works [46-47]. According to laboratory test results of Gaziantep limestone [47], some material characteristics are defined as mean unconfined compressive strength of 10.7MPa (in the range 3.7MPa to 67.4MPa), mean tensile strength of 3.8MPa (in the range 1MPa to 15.1MPa) and mean unit weight of 20.02kN/m³ (in the range 18.1 kN/m³ to 25.7 kN/m³). However, an emphasize should be given that estimation of strength of multicomponent masonry structure built with stone and mortar is a difficult task due to quite complex process of internal mechanism developed between stone and mortar [111-114]. Both the masonry unit and the mortar strength have a dominant effect on the mechanical behavior and failure mode in masonry constructions [115-117]. Hence, for simplicity, an isotropic and homogeneous model (macro model) that conform to previous studies [80-81] is assumed to prevail for structural modeling of masonry bridge in this study (i.e., Masonry stones and mortar are simulated with together regarding no clearance between masonry blocks and mortar.). It is reported [81] that the homogenized material of macro modeling presents simpler solutions for masonry structures. For estimation of strength of homogenized material properties of masonry unit, a composite material theory is mostly used in previous studies [78, 118-120] that proposes some empirical equations (compressive strength of mortar and stone) given by a basic form:

(3.2)

$$f_{c,mas} = a \cdot f_{c,st}^b \cdot f_{c,mo}^c$$

where $f_{c,mas}$ =compressive strength of masonry unit, $f_{c,st}$ =compressive strength of stone, $f_{c,mo}$ =compressive strength of mortar, a =classification coefficient of masonry unit, b =participation rate or volumetric ratio of stone/brick and c =participation rate of mortar. Thus, the formula of Eq. 3.2 is also used for estimation of compressive strength of masonry bridge in this article by putting some suitable coefficients ($a=0.8$, $b=0.7$ and $c=0.2$) conforming to the past works [121-124]. However, strength of mortar in this formula should be adequately accounted into estimations. For this issue, historical investigation of the compressive strengths of mortars of historical structures in a periodical order is studied in a past work [125] (Table 3.5). Since the stone is originated

from quarry stone (N1, Table 3.6) with the compressive strength of $f_{c,st}=38\text{MPa}$ (Table 3.6); the compressive strength of mortar $f_{c,mo}=2.5\text{MPa}$ is taken into account in this article on the basis of the observation of the moderate quality (IIa, Table 3.6) and the construction of historical period (between “Bezesteni” of 16th century and “Old house Mouson” of 19th century; Table 3.5). Consequently, the compressive strength (Eq.1) of masonry bridge is estimated as $f_{c,ma}=12.26\text{MPa}$ for critically (failure) evaluations under loading. In accordance with previous suggestion [5] that is consistent with earlier effort [46], the ratio of tensile strength to compressive strength ($f_{c,ma}$) of masonry bridge is presumed as 1/10 [121-124]. Critical places on the masonry bridge are determined by the failures limits of compressive and tensile strength of masonry unit (mentioned above) observed from stress distribution of masonry bridge.

Table 3.4 Proposed material properties [46].

Parameter	Value
Unit weight (kN/m^3)	18
Poisson ratio	0.15
Compressive strength (MPa)	38
Tensile strength (MPa)	3.8
Modulus of elasticity (Young's Modulus) (MPa)	1500

Table 3.5 Historical development of compression strength of mortar of historical structures [125].

Structure	Period	Compression strength in MPa
Roman Forum	2nd century	2.5-4.0
Galerius Palace	3rd century	3.0-4.5
Acheropiitos	5th century	2.3-3.0
Hagia Sophia	7th century	2.0-6.0
Hagios Panteleimonas	14th century	1.0-1.4
Hagia Aikaterini	13th century	1.6-2.0
Bezesteni	16th century	2.5-3.5
Old house Mouson	19th century	1.5-2.0

Table 3.6 Compression strength of mortar based on compression strength of stone and mortar group [126].

*Quality category	Stone compression strength (fc,st)	Mortar compression strength (fc,mo in MPa) regarding the mortar group			
		I	II	IIa	III
N1	≥ 20 MPa	0.6	1.5	2.4	3.6
	≥ 50 MPa	0.9	1.8	2.7	4.2
N2	≥ 20 MPa	1.2	2.7	4.2	5.4
	≥ 50 MPa	1.8	3.3	4.8	6.0
N3	≥ 20 MPa	1.5	4.5	6.0	7.5
	≥ 50 MPa	2.1	6.0	7.5	10.5

	≥ 100 MPa	3.0	7.5	9.0	12.0
N4	≥ 5 MPa	1.2	2.0	2.5	3.0
	≥ 10 MPa	1.8	3.0	3.6	4.5
	≥ 20 MPa	3.6	6.0	7.5	9.0
	≥ 50 MPa	6.0	10.5	12.0	15.0
	≥ 100 MPa	9.0	13.5	16.5	21.0
*Quality category can be defined by a general classification.	Quality category	General classification	Joint height to stone length	Angle of joint in $\tan\alpha$	Transfer factor η
	N1	Quarry stone masonry	≤ 0.25	≤ 0.30	≤ 0.50
	N2	Hammered coursed rubble masonry	≤ 0.20	≤ 0.15	≤ 0.65
	N3	Coursed rubble masonry	≤ 0.13	≤ 0.10	≤ 0.75
	N4	Ashlar masonry	≤ 0.07	≤ 0.05	≤ 0.85

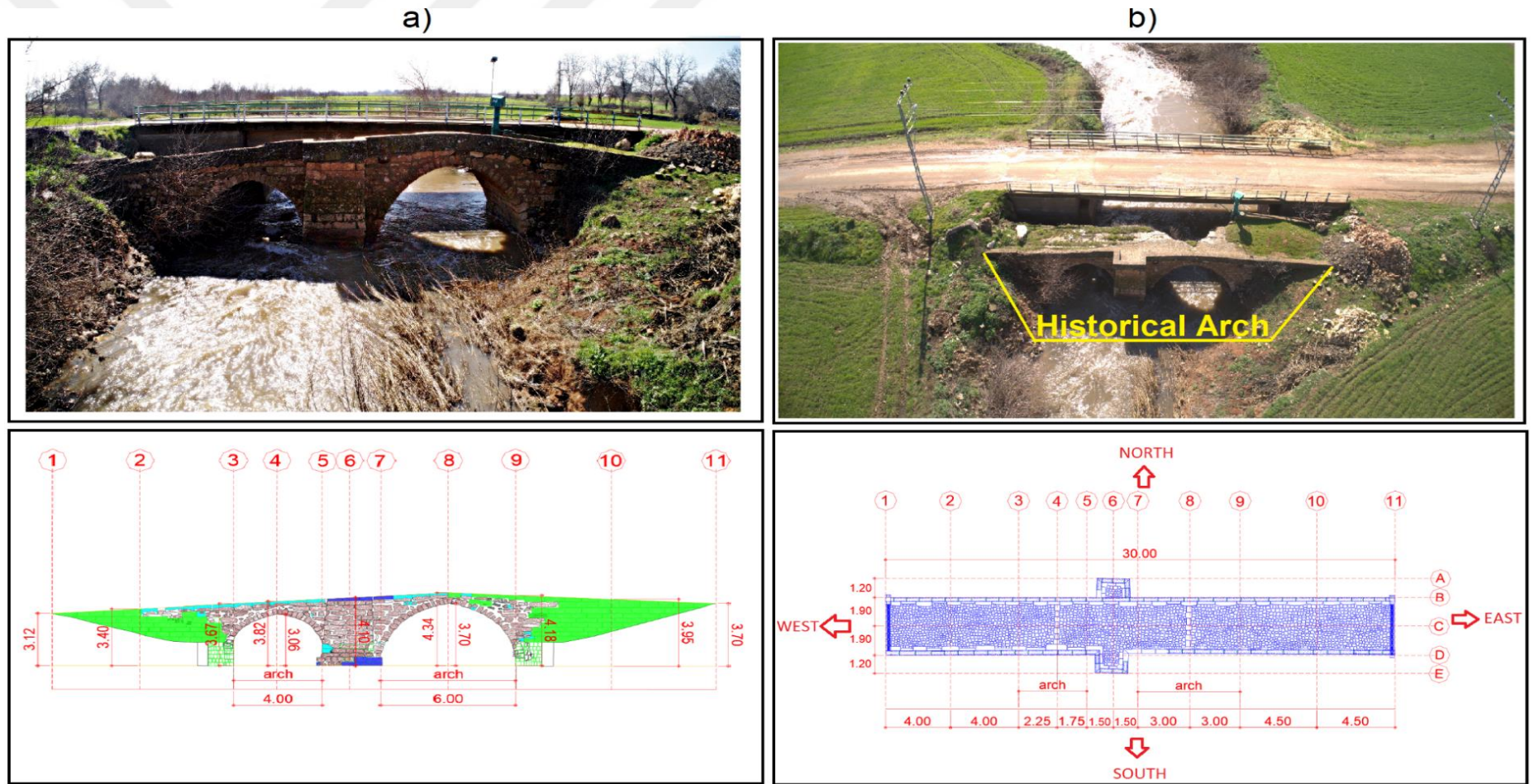


Figure 3.6 Investigated historical bridge in the study: a) General photograph of bridge, and front section views, b) Aerial photograph of bridge and top section views with dimensions of structural parts in west and north (modified from) [110].

It should be emphasized here that the stress distribution failures of the masonry bridge (and the substructure) are evaluated by considering the pressure and tensile strength limits of the stones above.

Table 3.7 Some proposed soil characteristics of bridge's substructure [127].

Parameter	Value
Unit weight (kN/m ³)	18
Compressive strength (MPa)	10
Tensile strength (MPa)	1
Modulus of elasticity (Young's Modulus) (MPa)	1000
Shear wave velocity (m/s)	400
Poisson ratio	0.15
Thickness (m)	30

The structural modeling of the masonry arch bridge in this study, according to the macro model, the structure is isotropic and homogeneous and it was assumed to be suitable with past studies [80-81]. In other words, masonry unit and mortar properties are considered as composite material (i.e., no clearance between masonry blocks and mortar) by homogenizing. It has been emphasized that macro modeling can be preferred for faster and easier solutions for large and complex masonry structures. in the past studies [81, 128].

The geotechnical properties of soil deposits generally play an important role in changing seismic ground motion [129]. As for the substructure (soil) conditions of bridge (Fig 3.6), the geological part of the bridge is formed by deposits of some lower limestone deposits, as well as deposits of undifferentiated quaternary parts and eocene neritic limestones [130] (Fig 3.6a).

Infrastructure of soil of bridge is composed of limestone deposits moderately weathered with the RQD values typically 43% [127] (Fig 3.6b), which is assumed to extend to a great depth some proposed soil characteristics of bridge's infrastructure employed in this study are given Table 3.7, which has been benefited from a past effort in the region [127]. Due to a homogenous deposit of sublayer (limestone) defined above, the sublayer of the bridge was modeled as a single layer with a thickness of 30m on the bedrock.

The choice of 30 m thickness may be that the surface layers located at a depth of almost 30 m are more affected by the strong ground motion reported in previous studies [129, 131-136]. As previously stated, 3D finite element modeling was used for bridge the structure and infrastructure through SSI analysis in this study. The 3D finite element modeling of bridge with fixed base (Fig 3.7a) and SSI with viscous dashpot (Fig 3.7b) are separately shown in Fig 3.7. The finite element model is prepared according to the modeling features and rules of the SAP2000 (v.20) [98] program. For both bridge and substructure constructions, solid elements with the shape of rectangular box that have 8 nodes and 6 degrees of freedom at each node were used for modeling in the study, on the basis of the previous recommendations [63, 90, 137-138]. During the FEM modeling of structure (bridge), 11336 solid elements with the size between 0.01m^3 and 1m^3 and 15213 points were used. For modeling of substructure (soil), 38996 solid elements including 53030 points were used. The dimensions of the solid element in substructure were varied from 1m^3 to 27m^3 which were constructed in more refinement as soil elements close to structure, in accordance with previous research [138].

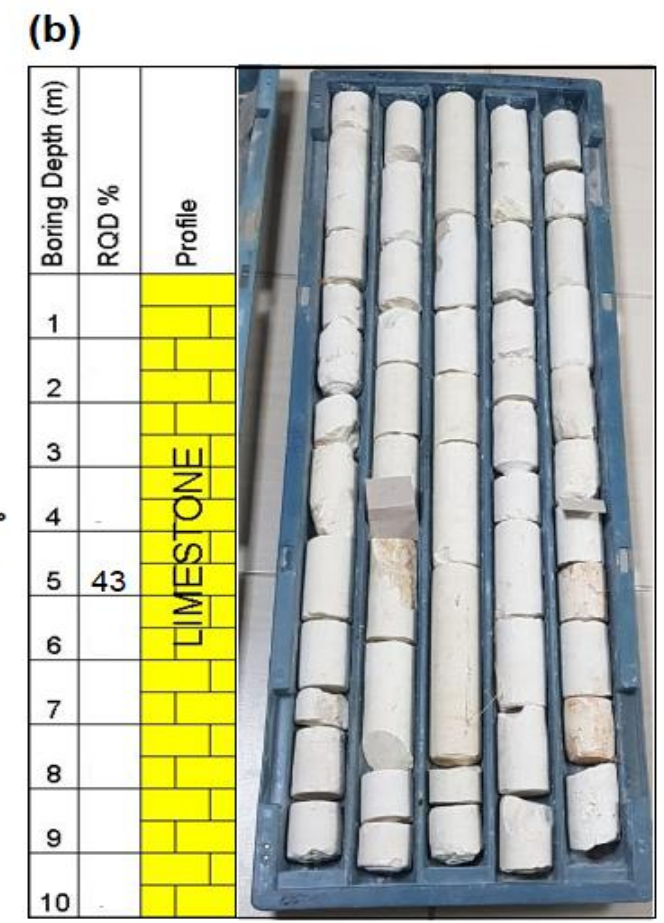
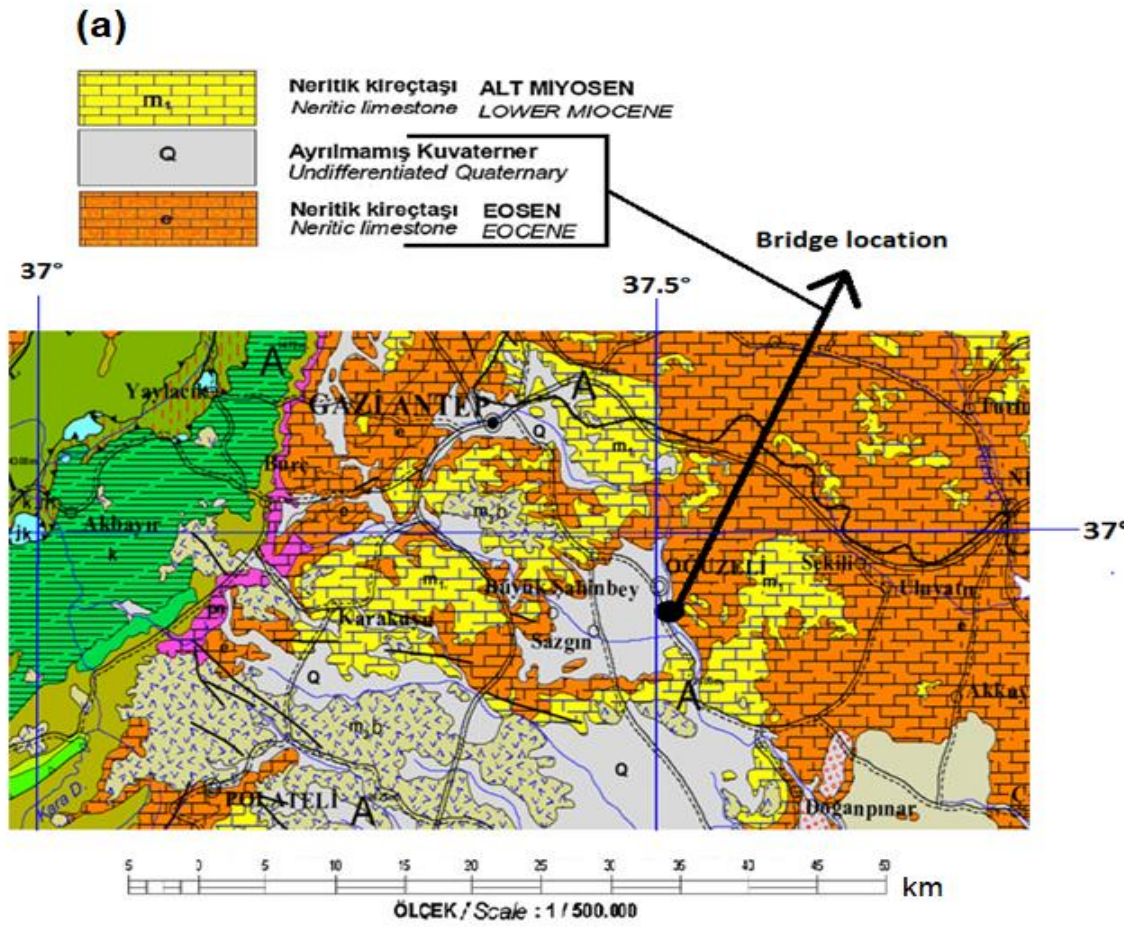


Figure 3.7 Infrastructure of the bridge: a) Geological map of region [130], b) A typical soil profile of bridge's infrastructure relating to RQD values [127].

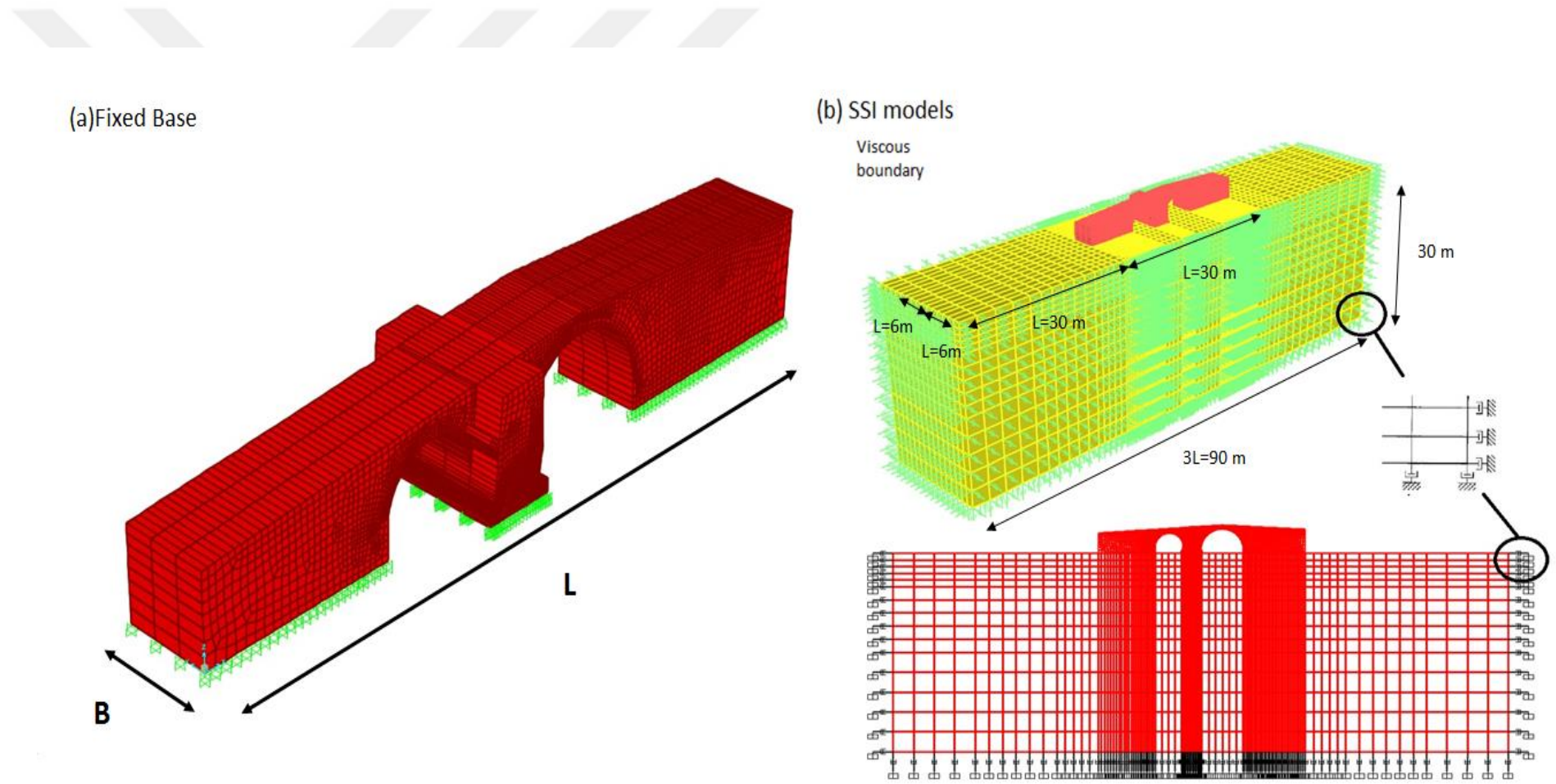


Figure 3.8 FEM of bridge and infrastructure: (a) FEM for fixed base of bridge (b) FEM for SSI of bridge and infrastructure with viscous dashpot (B= width of bridge, L=length of bridge, 3B =width of infrastructure (soil) boundary, 3 L=length of infrastructure (soil) boundary).

It has been reported that if the distance of center of structure to the finite element model boundary of substructure is within 3 to 4 times of the foundation radius in horizontal direction and 2 to 3 times of the foundation radius in vertical direction, the effects of reflective waves are insignificant enough to be suitable for infrastructure modeling. [35, 139]. Moreover, in a parametrically investigation [139] in plan, the wave effects (in particular with consideration of base shear, and displacement) were found similar for the boundary length/structure length from 3 to 4.5 and boundary width/structure width from 2 to 3. In accordance with the past studies [35, 139], both the boundary length/structure length and boundary width /structure width equal to 3 in plan were used in this study, as shown in Fig 3.7. As mentioned before, for both infrastructure and bridge, the properties of homogeneous and isotropic materials are assumed by taking linear stress-strain behavior due to time-history analysis of the earthquake movement. The damping ratio (i.e., material damping) of the SSI system was taken to be 5% in the estimations for fixed based and SSI. The SSI analysis has been applied without foundation embedment between bridge and soil in accordance with the previous works [90, 138].

CHAPTER 4

RESULTS AND DISCUSSION

4.1 Influences of SSI Modeling

SSI influences comparatively with the fixed base solution and the effects of near-fault and far-fault earthquakes are illustrated in the figures (Figs.4.1-4.3) given for the amplitudes (acceleration, velocity, displacement) (Fig.4.1), spectral responses (spectral amplifications and periods) of response spectrums (Fig.4.2) and stress distributions (tensile, compressive) (Fig.4.3). The plots of amplitudes and response spectrums (Figs.4.1-4.2) are typically drawn for the critical points (i.e., maximum tensile stresses shown in Fig.4.3). The response spectrums (Fig.4.2) are also presented by design spectrum in accordance with TSC (2007) [140]. The SSI influences in the peak amplitudes (Table 4.1a), peak spectral acceleration ratios ($S(T)$) and spectral periods (i.e., characteristic periods by design spectrum due to TSC (2007) [140] and predominant periods) (Table 4.1b) and critical stresses (i.e., maximum stresses of tension and compression) (Table 4.1c) are summarized in Table 4.1 including some additional points at structural elements at the bridge. Earthquake responses (from Table 3.1 and Fig.3.3) are also illustrated in Fig.4.2 (earthquake spectrum) and summarized in Table 4.1 for performance comparisons of specifically amplifications and resonance.

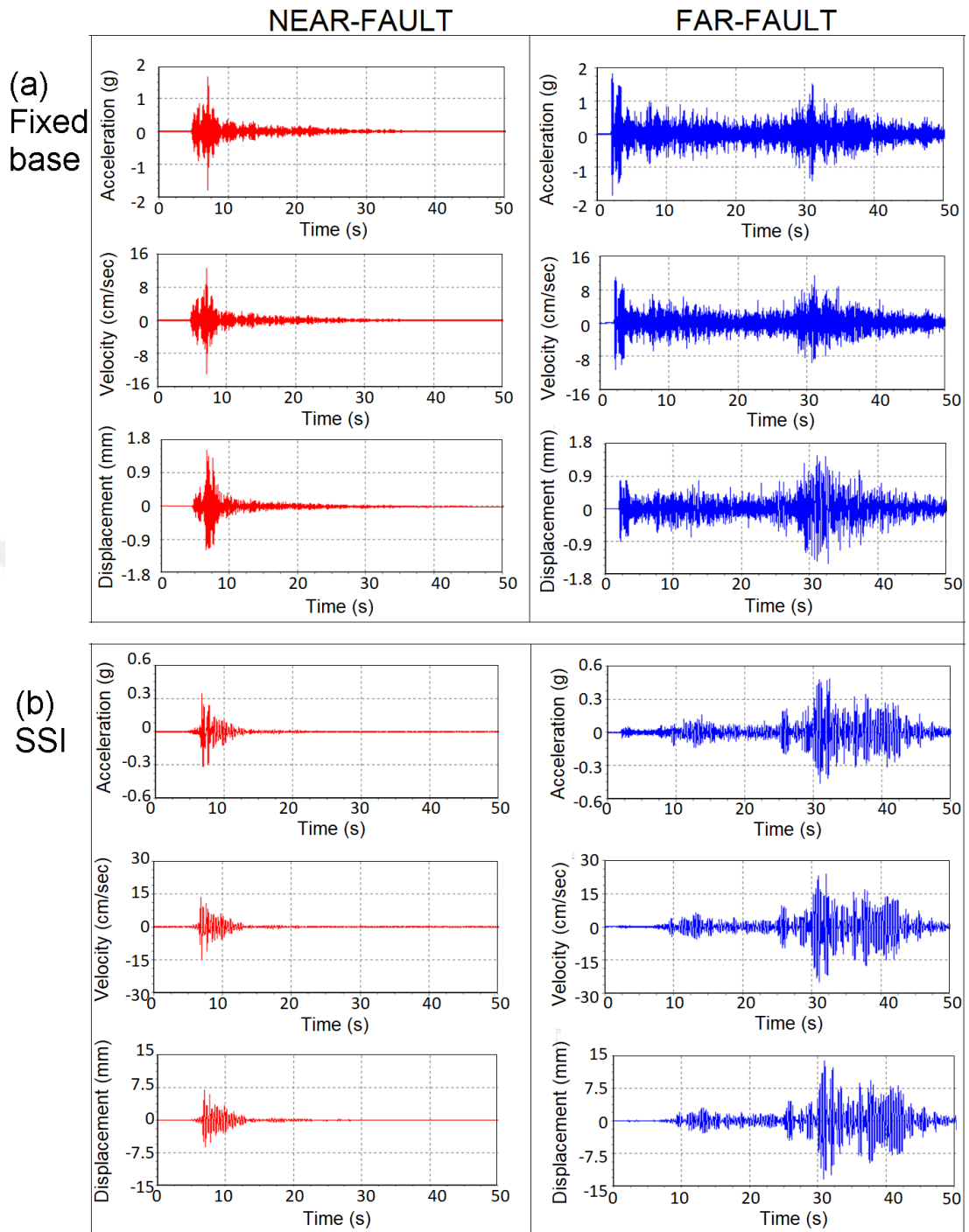


Figure 4.1 SSI influences for the amplitudes (typically at the critical point for the big arch at the inner top): a) fixed base solution, and b) SSI analysis.

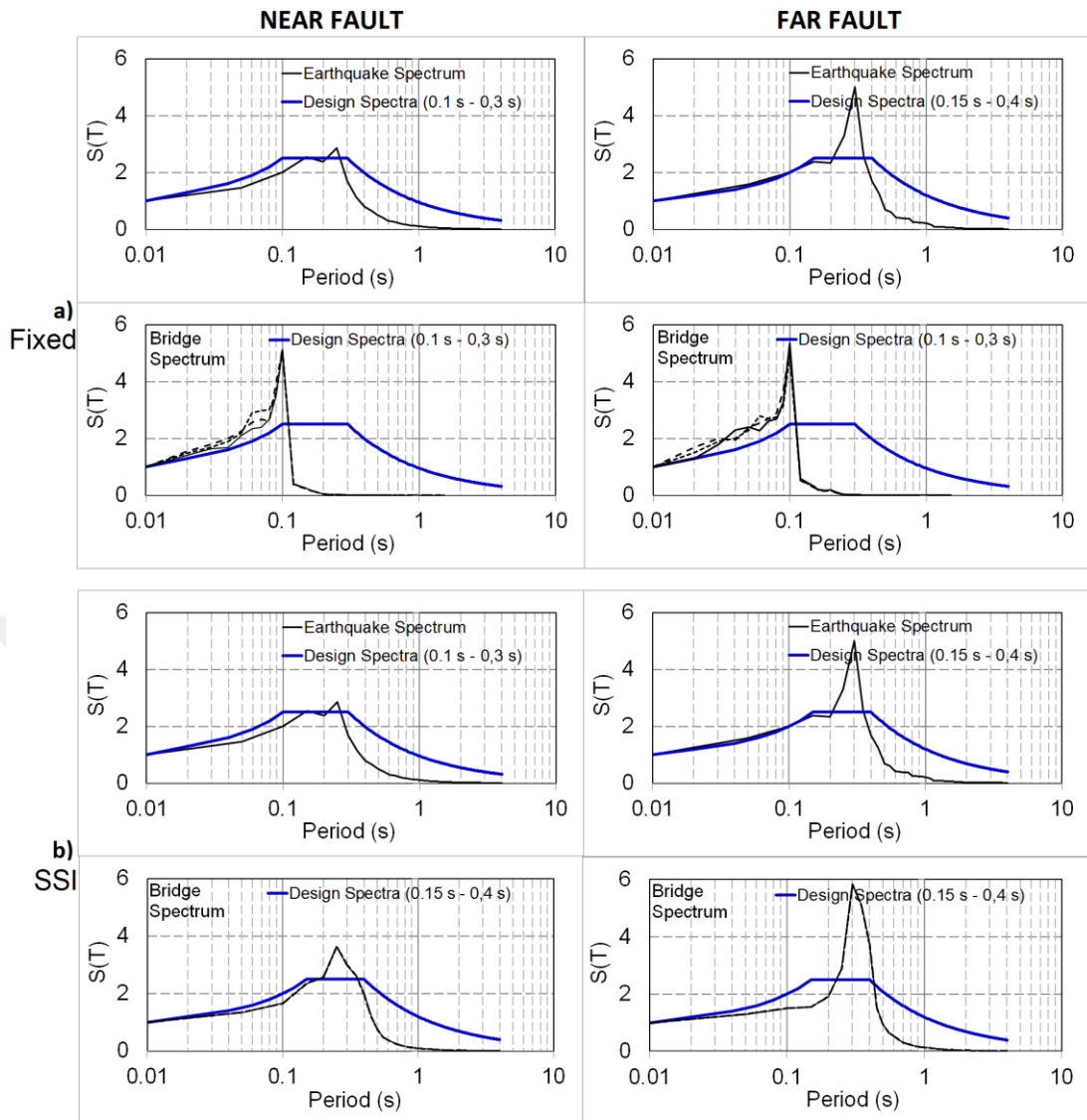


Figure 4.2 SSI influences for spectral responses of response spectrums (typically at the critical points for the big arch at the inner top, small arch at the inner top and pier at left upper): a) fixed base solution, and b) SSI analysis. i) $S(T)$ =Spectral acceleration ratio or spectral amplification; ii) Design spectrum in accordance with TSC (2007) [140]; Spectral acceleration ratio ($S(T)$ =normalized spectral acceleration to peak acceleration).

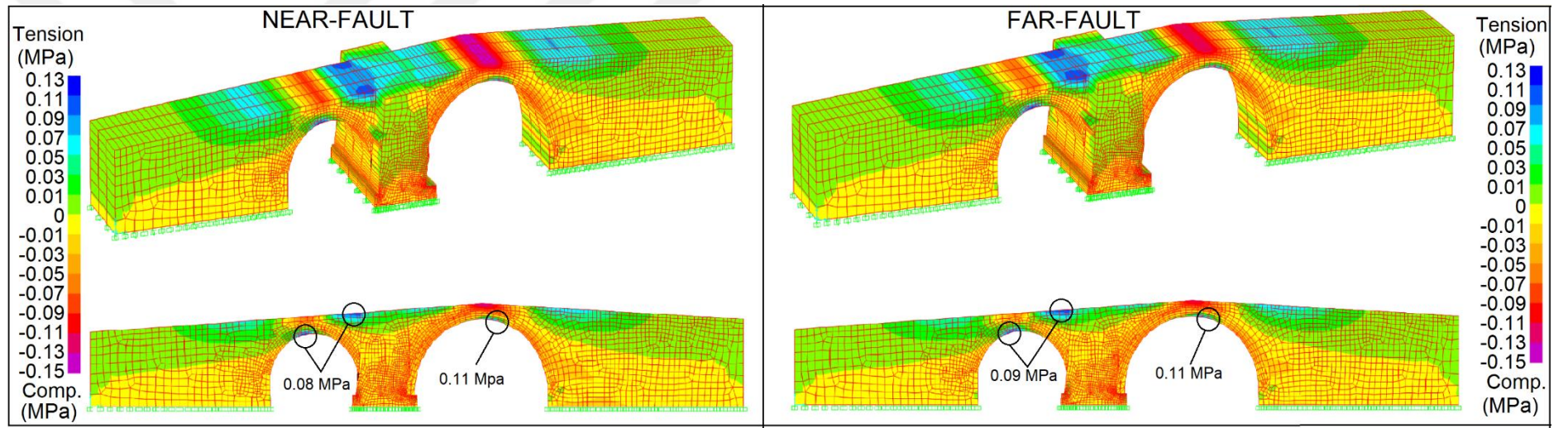


Figure 4.3(a) Fixed base solution.

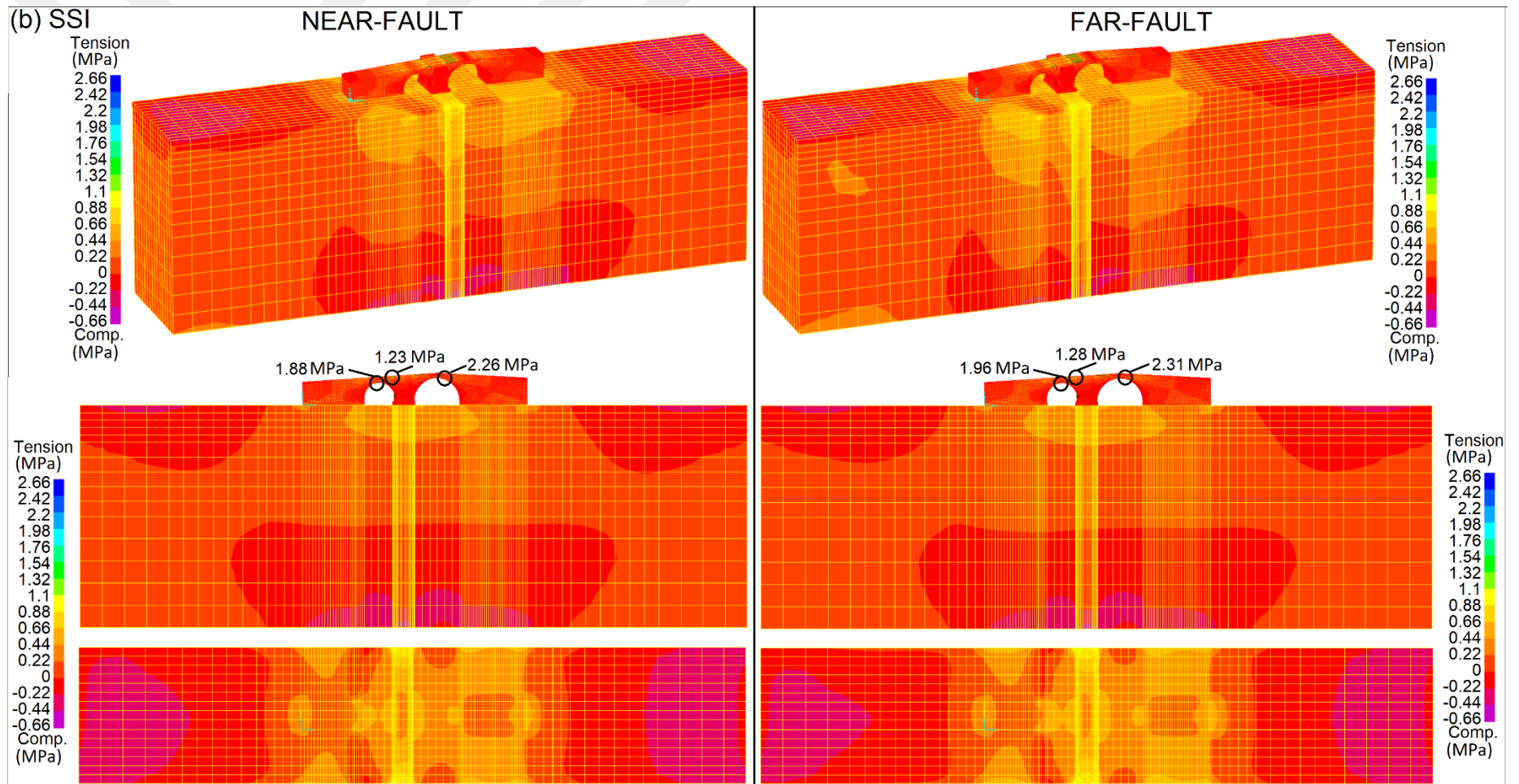


Figure 4.3(b) SSI analysis.

Table 4.1 Comparison of SSI and with fixed base.

Model		Fixed Base		SSI Analysis	
		Near-Fault Earthquake	Far-Fault Earthquake	Near-Fault Earthquake	Far-Fault Earthquake
Bridge responses*					
(a) Amplitude					
acceleration (g)	small arch (inner top)	1.28	1.31	0.32	0.46
	pier (left top)	1.76	1.85	0.34	0.48
	big arch (inner top)	1.79	1.84	0.34	0.48
	small arch (top)	0.92	0.95	0.33	0.47
	pier (right top)	1.98	2.08	0.35	0.49
	big arch (top)	1.04	1.05	0.35	0.49
velocity (cm/s)	small arch (inner top)	9.33	8.38	13.88	23.65
	pier (left top)	12.52	11.15	14.56	24.81
	big arch (inner top)	12.87	11.52	14.68	25.06
	small arch (top)	6.65	5.95	14.21	24.21
	pier (right top)	14.01	12.48	14.75	25.14
	big arch (top)	7.62	6.88	14.87	25.39
displacement (mm)	small arch (inner top)	1.2	1.1	6.6	13
	pier (left top)	1.5	1.5	6.9	13.7
	big arch (inner top)	1.5	1.5	6.9	13.8
	small arch (top)	0.8	0.1	6.8	13.4
	pier (right top)	1.6	1.6	7	13.8
	big arch (top)	0.9	0.9	7	14
(b) Spectral responses of response spectrum					

spectral acceleration ratio (S(T))	small arch (inner top)	5.14	5.35	3.6	5.8
	pier (left top)	5.11	5.16	3.6	5.8
	big arch (inner top)	5.14	5.28	3.6	5.8
	small arch (top)	5.13	5.27	3.7	5.8
	pier (right top)	5.11	5.14	3.6	5.8
	big arch (top)	5.16	5.43	3.6	5.8
	Average	5.13	5.27	3.62	5.8
predominant period (s)	small arch (inner top)	0.1	0.1	0.25	0.3
	pier (left top)	0.1	0.1	0.25	0.3
	big arch (inner top)	0.1	0.1	0.25	0.3
	small arch (top)	0.1	0.1	0.25	0.3
	pier (right top)	0.1	0.1	0.25	0.3
	big arch (top)	0.1	0.1	0.25	0.3
range of characteristic periods by design spectrum (s)	small arch (inner top)	0.10-0.30	0.10-0.30	0.15-0.40	0.15-0.40
	pier (left top)	0.10-0.30	0.10-0.30	0.15-0.40	0.15-0.40
	big arch (inner top)	0.10-0.30	0.10-0.30	0.15-0.40	0.15-0.40
	small arch (top)	0.10-0.30	0.10-0.30	0.15-0.40	0.15-0.40
	pier (right top)	0.10-0.30	0.10-0.30	0.15-0.40	0.15-0.40
	big arch (top)	0.10-0.30	0.10-0.30	0.15-0.40	0.15-0.40
(c) maximum stress					
	tension (MPa)	0.11	0.11	2.26	2.31
	compression (MPa)	0.14	0.14	0.65	0.65

Earthquake**

Near-Fault

Far-Fault

Amplitude	acceleration (g)	0.26	0.24
	velocity (cm/s)	10.26	8.97
	displacement (mm)	5.2	5
Spectral responses	spectral acceleration ratio (S(T))	0.74	1.2
	predominant period (s)	0.25	0.3
	range of characteristic periods by design spectrum (s)	0.15-0.40	0.15-0.40

*Responses from Figs.4.1-4.3 and corresponding locations

**Responses of near and far-fault earthquakes from Fig.3.3 (Table 3.1) (assumed bedrock motions) and corresponding spectrums (Fig.4.2)

As concerned with the amplitudes (Fig.4.1, Table 4.1a), it is found that the earthquakes responses can be modified (increase or decrease) by SSI analysis when compared with fixed base. It is seen that the SSI analysis yields to different responses in comparison with fixed base under earthquake motion (for both near-fault and far-fault motion). While the effect of accelerations become relatively prominent due to the fixed base analysis (nearly up to 2g), the SSI analysis results in relatively less accelerations (nearly up to 0.5g). On the other hand, fixed based solutions estimate less displacement nearly up to 2mm, while the displacements by SSI can be extended to nearly 15mm. As a result, the accelerations are limited due to SSI influences, while the displacements are increased. Hence, a deformation of considerable influence by 15mm displacement due to SSI effect could be expected at the bridge when examined the displacement results in historical structures studied in a past study [124]. The results are due to a clear fact that disregarding the dynamic stiffness of the surrounding soil especially below founded soil in fixed base solution can lead to significant deviations from SSI analysis [141]. It is noticed that flexibility of the understructure of soil could have a important role on the amount of amplitudes due to the SSI effect. [57, 142]. On the comparison of near and far-fault motions, it is observed from the amplitudes that the far-fault motion due to SSI influences results in larger responses than the ones of near-fault motion. This shows that the far-fault motion should not be underestimated specifically for evaluating SSI influences.

In regard to the spectral responses of response spectrums (Fig.4.2, Table 4.1b), it is found that spectral amplifications ($S(T)$) are obtained relatively high (i.e., $S(T) > 2.5$) upper limit of design spectrum recommended by TSC (2007) [140] by the fixed base and SSI influences in both. The amplification of fixed base can be reduced by SSI influence only for the near-fault motion. However, it could be noted that the bridge specifically due to the SSI influences is more responded by far-fault earthquake similar to amplitude responses, compared to near-fault motion. It is well known (TSC, 2007) [140] that spectral amplifications greater than $S(T) = 2.5$ can be considered dangerous potentially leading to significant damage on structures. Thus, the historical bridge studied in this study could be considerably vibrated due to a possible earthquake for the region. The high spectral vibrations obtained for the bridge could be attributed to stiffness of structure and/or soil rather than magnitude of earthquake accelerations. As for the spectral periods (Fig.4.2, Table 4.1b), the bridge with fixed case vibrates in the

predominant periods of 0.1s or in the characteristics periods of 0.1s-0.30s (in accordance with design spectrum TSC (2007) [140]). On the other hand, the bridge under SSI influences rises the spectral periods to the predominant periods of 0.25s-0.30s or to the characteristics periods of 0.15s-0.40s due to design spectrum. It is observed from the fixed and SSI cases, both the near and far-fault motions produce similar magnitudes in the spectral periods. The obtained spectral periods for both the fixed and SSI cases appear reasonable, since the bridge can be considered as low-rise structure. The increased predominant periods due to SSI influences in comparison with fixed case may be attributed to flexibility of bridge-soil system and soil characteristics of substructure reported in past studies [143-144] As observed the spectral responses due to SSI effects in previous works, while the spectral accelerations are in a trend of decrease [138], the predominant periods are found to increase [142-144].

For determining a possibility of resonance effect based on response spectrums (Fig.4.2, Table 4.1b), the predominant periods or characteristics periods (design spectrum) of the bridge (for fixed and SSI) discussed above can be compared with the ones of earthquake vibration (i.e., predominant periods of 0.25s-0.3s, characteristics periods of 0.15s-0.40s). From the comparisons (for the near and far-fault effects in both), it is appeared that earthquake motion and bridge are vibrated at different predominant periods or characteristics periods due to fixed base solution without proposing a resonance effect in strong evidence. On the other hand, the bridge and earthquake motion due to SSI influences are vibrated at similar predominant periods or characteristics periods indicating to a resonance case in strong evidence. In consistent with this finding, the SSI influences are also reported to be significant on the resonance in past studies [138, 145]. Hence, investigation of the historical bridge by the SSI modeling is of significant for understanding a possibility of various adverse effects.

As for the effects on stress distributions (tension, compression) (Fig.4.3, Table 4.1c), it is seen that the near-fault and far-fault motions lead to similar responses of stress distribution as well as maximum stresses in both the fixed and SSI cases. Thus, as implied earlier (from the results of amplitude and response spectrum), the far-fault earthquake could become a significant effect as much as near-fault earthquake on the bridge responses. In comparison with fixed base solution, it is clearly displayed from the stress distributions that regarding the SSI influences into seismically estimation of

bridge response results in larger stress than the ones of fixed base. The increased SSI influence is consistent with past works [62, 146]. As assessed earlier, the compressive strength of masonry bridge is critically considered as $f_{c,ma}=12.26\text{MPa}$, while the tensile strength of masonry bridge can be critically taken as 1/10 of compressive strength (i.e., tensile strength= 1.226MPa) into computation for the possibility of structural damage or failure. From the stress distribution (Fig.4.3), it is observed that tensile stresses could potentially become critical for damage (i.e., $>1.226\text{MPa}$), while the bridge can be considered stable under the compressive stresses (i.e., $<12.26\text{MPa}$). On the evaluation of critical stresses (based on tensile stresses), maximum stresses (tensile stress) obtained by fixed base solution (Fig.4.1a, Table 4.1c) are not found to reach to the critical stress level (i.e., $<\text{tensile strength}=1.226\text{MPa}$) in order for potentially causing a damage on the bridge. On the other hand, maximum stresses (tensile stress) computed by SSI influences (Fig.4.1b, Table 4.1c) exceed the critical stress level (i.e., $>\text{tensile strength}=1.226\text{MPa}$) that potentially offer a damage or failure. This clearly indicates that disregarding SSI solution for seismically concern computation of the historical bridge in this study could result in a misleading result in unsafe side. As shown from the stress distribution of SSI (Fig.4.1b), the critical stresses (i.e., tensile stress) are developed in the structural elements of small arch, pier and big arch similar to many arch works previously studied. From this, it is clear that the arches (as main part of masonry structural system) under the critical stresses (tensile stresses) could easily address crack regions and probable damage (similarly reported for different works [146] under a possible earthquake excitation. Thus, the bridge should be protected by performing necessary restoration.

4.2 Spectral responses by microtremor measurements

Response spectrums obtained by microtremor measurements are illustrated in Fig.4.4 for bridge and in Fig.4.5 for bridge's base, soil and bedrock. Shown in Fig.4.4, response spectrums of bridge are presented for the estimation methodologies i) by horizontal to vertical spectral ratio (HVSr, Nakamura technique) (Fig.4.4a), ii) horizontal spectral ratio of bridge to soil (HSR(soil), [73] (Fig.4.4b) and iii) horizontal spectral ratios of bridge to base of bridge (HSR(base), [73] (Fig.4.4c), as stated earlier. Spectral responses (i.e., spectral amplification, predominant (fundamental) frequency and predominant period) of bridge estimated from the response spectrums of

microtremor (Fig.4.4) are tabulated in Table 4.2 for HVSR (Nakamura), HSR(soil) and HSR(base) [73]. Spectral responses of bridge's base, soil and bedrock are also included in Table 4.2. In order for understanding the performances of the HSR estimations [73], the spectral responses of HVSR versus HSR(soil) and HSR(base) are illustrated in scattering plot in Fig.4.6 for amplification (Fig.4.6a) and predominant period (Fig.4.6b).



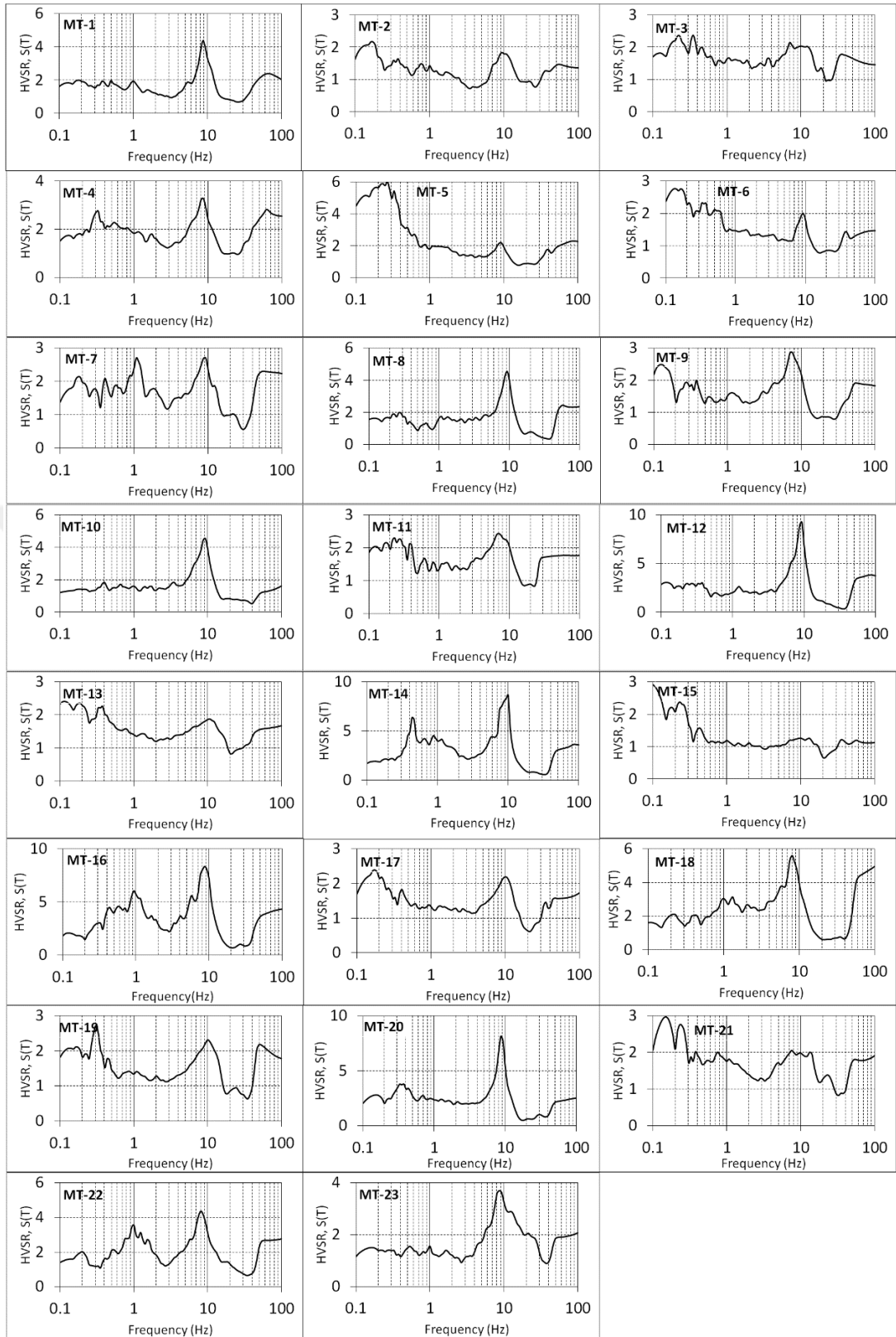


Figure 4.4(a) Horizontal to vertical spectral ratio (HVSr, Nakamura technique).

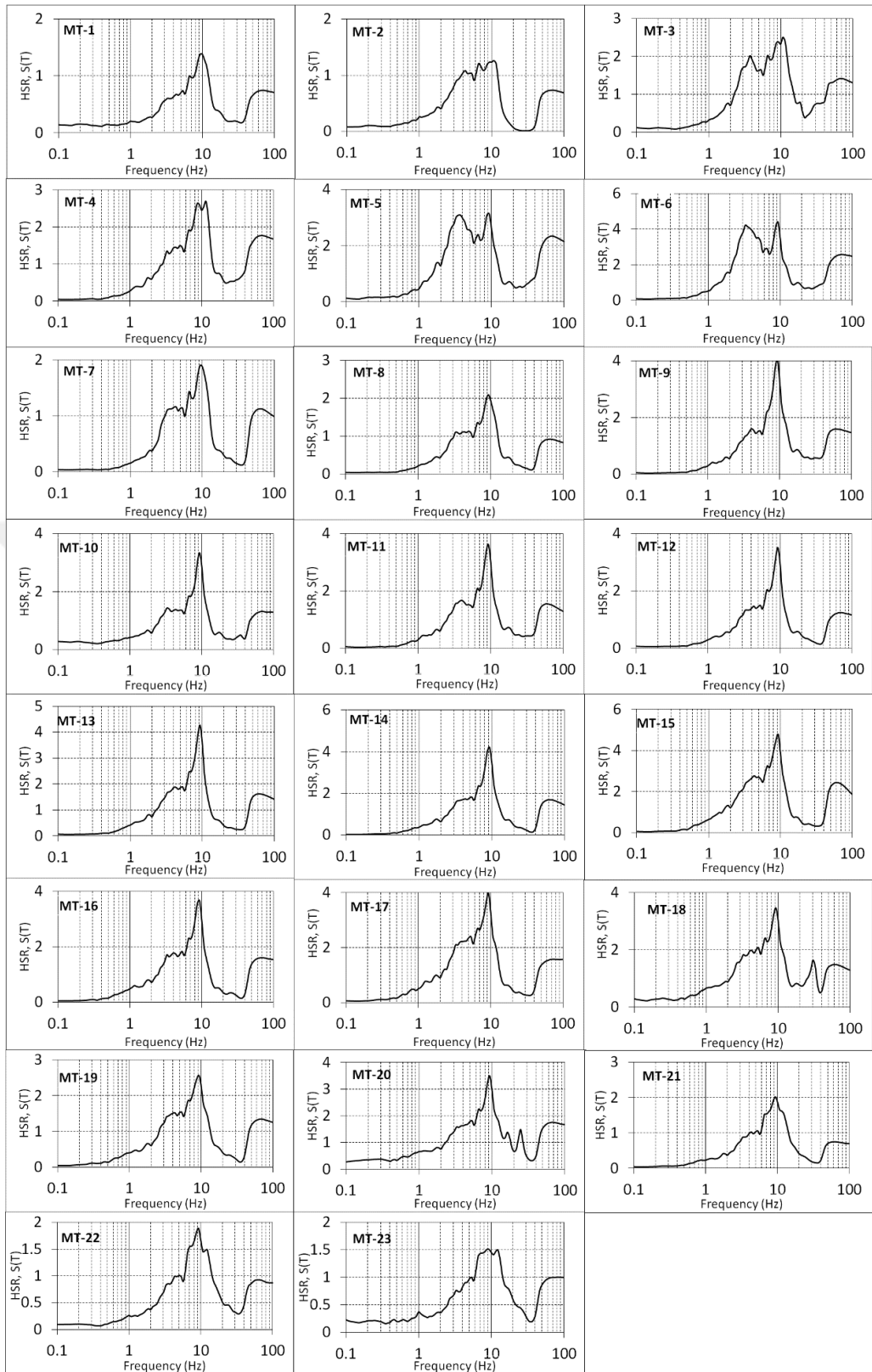


Figure 4.4(b) Horizontal spectral ratio of bridge to soil (HSR(soil)), [73].

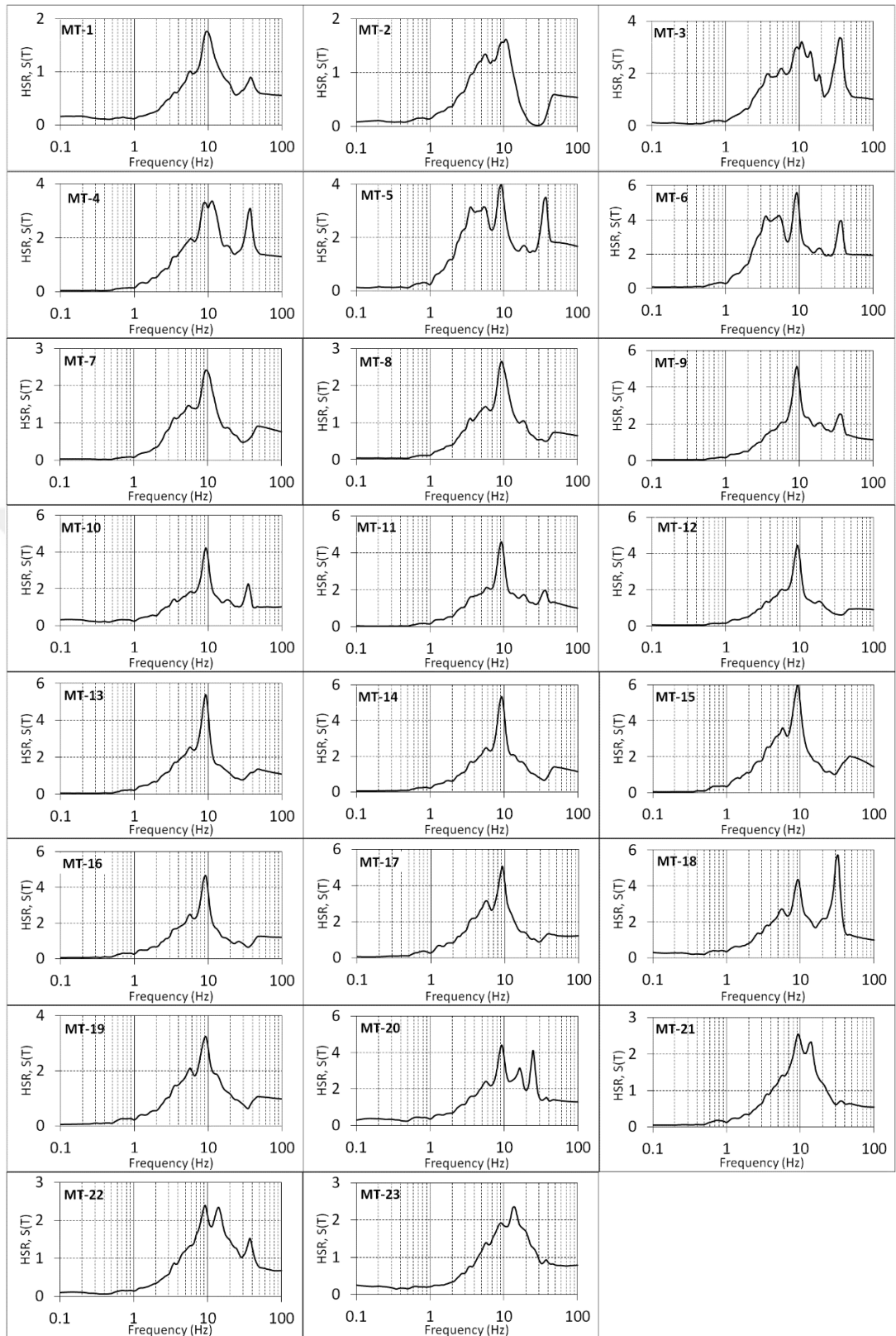


Figure 4.4(c) Horizontal spectral ratios of bridge to base of bridge(HSR(base), [73].

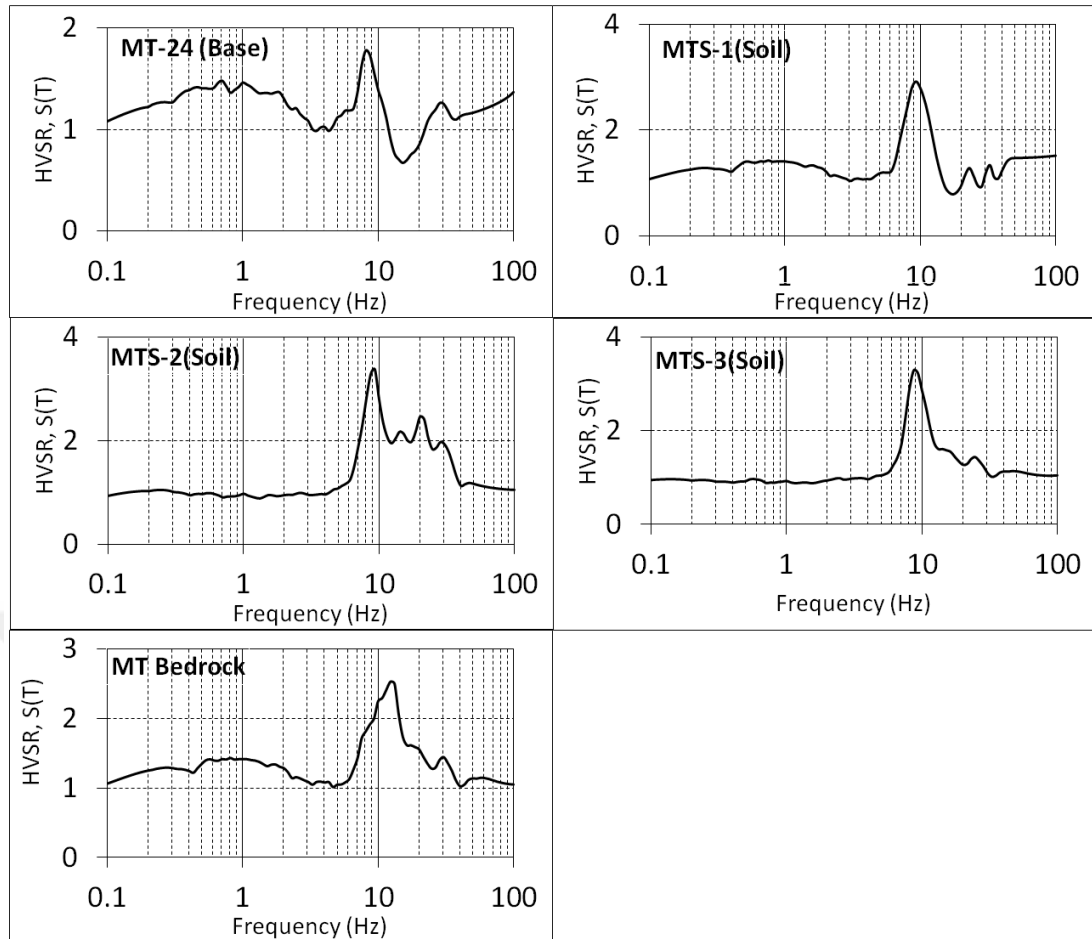


Figure 4.5 Response spectrums obtained by microtremor measurements for bridge's base, soil and bedrock.

Table 4.2 Spectral responses (spectral amplification, predominant (fundamental) frequency and predominant period) of bridge obtained from microtremor measurements using the estimation methodologies of HVSR (Nakamura's technique), HSR(soil) and HSR(base) [73] (Responses of bridge's base (mt24 base), soil (mts-1, mts-2, mts-3) and bedrock (mt bedrock) are also included for HVSR).

Methodology		HVSR (Nakamura)			HSR(soil) (Gosar, 2010)			HSR(base) (Gosar, 2010)		
Microtremor point	S(T)	fp (Hz)	Tp (s)	S(T)	fp (Hz)	Tp (s)	S(T)	fp (Hz)	Tp (s)	
MT-1	4.35	8.71	0.11	1.38	9.33	0.11	1.75	9.33	0.11	
MT-2	1.91	9.66	0.10	1.26	10.72	0.09	1.62	10.72	0.09	
MT-3	1.51	7.78	0.13	2.49	10.72	0.09	3.21	10.72	0.09	
MT-4	3.27	8.44	0.12	2.68	11.50	0.09	3.35	11.50	0.09	
MT-5	2.17	8.69	0.12	3.14	9.33	0.11	3.97	9.33	0.11	
MT-6	1.99	9.32	0.11	4.39	9.33	0.11	5.56	9.33	0.11	
MT-7	2.67	9.32	0.11	1.90	9.33	0.11	2.41	9.33	0.11	
MT-8	4.53	9.27	0.11	2.09	9.33	0.11	2.65	9.33	0.11	
MT-9	2.85	7.36	0.14	4.04	9.33	0.11	5.12	9.33	0.11	
MT-10	4.5	9.05	0.11	3.34	9.33	0.11	4.23	9.33	0.11	
MT-11	2.43	7.16	0.14	3.63	9.33	0.11	4.60	9.33	0.11	
MT-12	8.96	8.81	0.11	3.52	9.33	0.11	4.45	9.33	0.11	
MT-13	1.86	10.72	0.09	4.26	9.33	0.11	5.39	9.33	0.11	
MT-14	8.64	10	0.1	4.21	9.33	0.11	5.34	9.33	0.11	
MT-15	1.26	13.21	0.08	4.76	9.33	0.11	6.02	9.33	0.11	
MT-16	8.32	8.69	0.11	3.67	9.33	0.11	4.65	9.33	0.11	
MT-17	2.19	10	0.10	3.99	9.33	0.11	5.05	9.33	0.11	
MT-18	5.51	7.89	0.13	3.45	9.33	0.11	4.37	9.33	0.11	
MT-19	2.31	10	0.10	2.56	9.33	0.11	3.24	9.33	0.11	
MT-20	8.04	8.84	0.11	3.49	9.33	0.11	4.41	9.33	0.11	
MT-21	2.05	7.56	0.13	2.01	9.33	0.11	2.55	9.33	0.11	
MT-22	4.3	7.99	0.13	1.89	9.33	0.11	2.39	9.33	0.11	

MT-23	3.62	9.17	0.11	1.51	8.70	0.11	2.34	14.17	0.07
Average	3.88	9.02	0.11	3.02	9.51	0.10	3.85	9.75	0.10
MT-24 (Base)	1.76	8.26	0.12						
MTS- 1(soil)	2.88	9.4	0.11						
MTS- 2(soil)	3.31	9.17	0.11						
MTS- 3(soil)	3.44	8.94	0.11						
MT Bedrock	2.5	13.21	0.08						

S(T)=spectral amplification or spectral acceleration ratio; fp=predominant (fundamental) frequency); Tp=predominant period

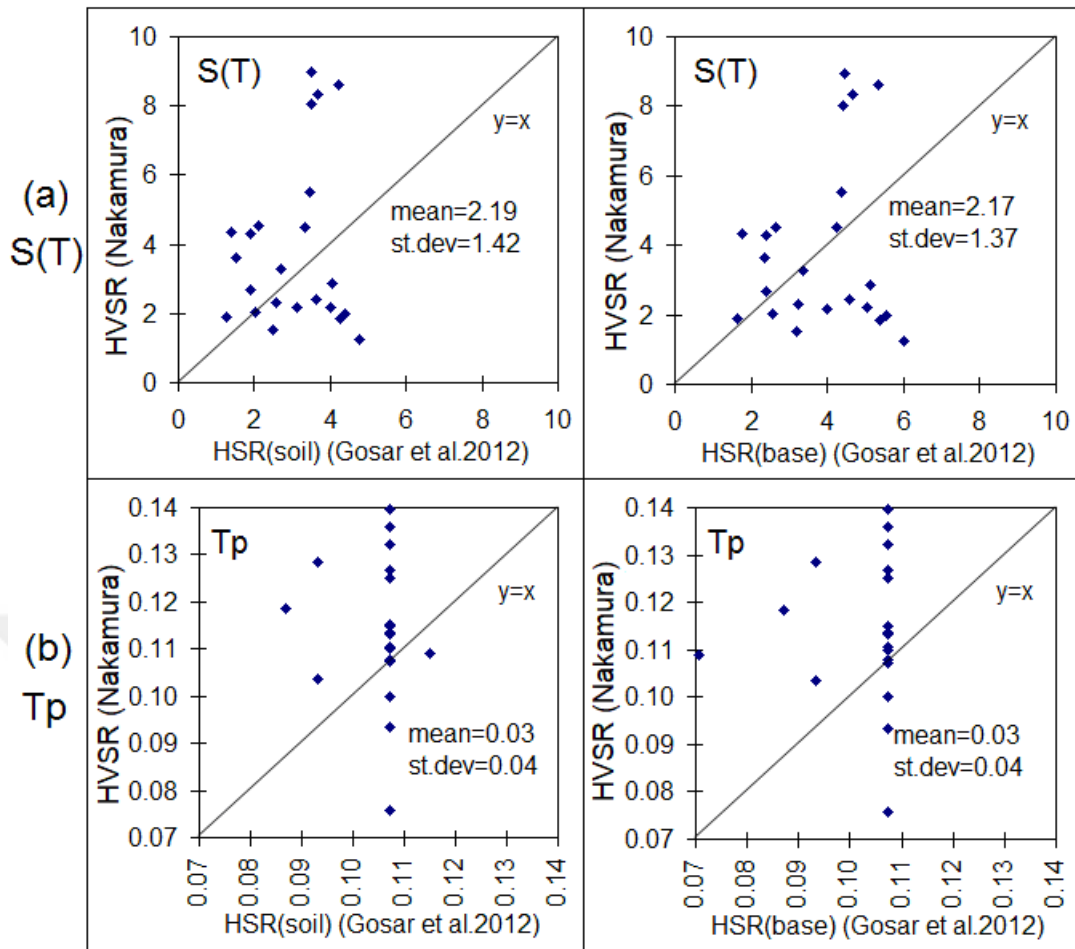


Figure 4.6 HVSR versus HSR(soil) and HSR(base) for: a) amplification (S(T), and b) predominant period (Tp) (y=x means perfect fit; mean and standard deviation are estimated from residuals).

As shown from the responses (Fig.4.4, Table 4.2), amplifications of bridge due to the estimations are obtained in the range 1.51-8.96 by average of 3.88 (HVSR Nakamura), 1.26-4.76 by average of 3.02 (HSR(soil)) and 1.62-6.02 average of 3.85 (HSR(base)). As for the predominant periods, they are obtained in the range 0.08s-0.14s by average of 0.11s (HVSR Nakamura), 0.09s-0.11s by average of 0.10s (HSR(soil)) and 0.07s-0.11s by average of 0.10s (HSR(soil)). It is understood from the results that the spectral responses by the three methodologies are generally offered within similar ranges. Even though their responses (specifically spectral amplifications) are in different magnitudes in a scattering, they mostly appear to produce similar trend of influence (increase or decrease) to figure out the bridge's response. It can be generally said that the bridge at majority of locations negatively offers high spectral amplifications (S(T)) that exceed the proposed upper limit of design spectrum due to TSC (2007) [140] (i.e.,

$S(T) > 2.5$). In addition, the predominant periods (T_p) of bridge are obtained in low periods that seem reasonable for low-rise structures like the historical bridge in this study. As a preliminary observation, the high spectral amplifications (Table 4.2) appear in a matching with the ones of the fixed base solution and SSI analysis in both (Table 4.1). Whereas the predominant periods (Table 4.2) seem more consistent with the ones of fixed base solution compared to SSI analysis (Table 4.1). However, a comparison in detail (location by location) will be carried out in the next section for a robust analysis. From the average values of responses (Table 4.2), it can be felt that the estimations due to HVSR and HSR(base) are more able to produce similar results compared to HSR(soil). However, it should be emphasized that the employed three estimation methodologies do not always guarantee for similarly responding. Moreover, they may offer the responses in a wide range of scattering. Thus, their results would be more beneficial for spectral contributions when used all together as stated above.

As concerned with HVSR versus HSR(soil) and HSR(base) (Fig.4.6), an emphasize should be given that confirmation the fitting based on the statistics of correlation coefficient may fail to demonstrate model inadequacies and data characteristics [147; 148] such as the data evaluations by ambient vibrations. Alternatively, confirmation could be strongly recommended by the residuals in mean for accuracy and in standard deviation (st.dev) for precision [149]. Clearly, the lower the values of mean and standard deviation, the better the model performance. From the scattering plots (Fig.4.2a, Fig.4.2b), it can be said that that both HSR(soil) and HSR(base) appear to perform the responses in similar accuracy (mean) and precision (st.dev). Regarding the proposed design limit of $S(T)=2.5$ of seismic code (TSC, 2007) [140], their accuracy and precision (specifically for amplification) could be considered to moderately fit HVSR (Nakamura) method. Thus, both the methods HSR(soil) and HSR(base) are valuable to assist Nakamura method for assessment of spectral responses. As can be observed from the scattering plots (Fig.4.2), some spectral responses in accuracy and precise are significantly deviated from perfect line ($y=x$). On the other hand, all remaining ones are accumulated in a reasonable deviation. Thus, this qualitative observation of HVSR versus HSR(soil) and HSR(base) could increase accuracy of estimations for spectral responses obtained by these methodologies. Next, the microtremor results (due to Nakamura method) are comparatively presented with

SSI and fixed base analysis under the effects of near and far-fault earthquakes for suitability of bridge model.

4.3 Comparison of microtremor measurements with SSI and fixed base analysis

For understanding the capability (suitability) of bridge modeling, microtremor measurements (using Nakamura technique) are compared with SSI analysis and fixed base model under the effects of near and far-fault earthquakes for the spectral responses (spectral amplifications, predominant periods) in Figs.4.7-4.8. Results by Nakamura technique only are employed for comparison of microtremor measurements, since it is the most common estimation method used in practice stated earlier. As a result of the comparisons of spectral accelerations of microtremor measurements the closest values to Nakamura was observed to be the SSI far fault earthquakes (Fig. 4.7) and the results of comparisons of predominant periods of microtremor measurements the closest values are the fixed base point under near and far fault earthquakes (Fig. 4.8).

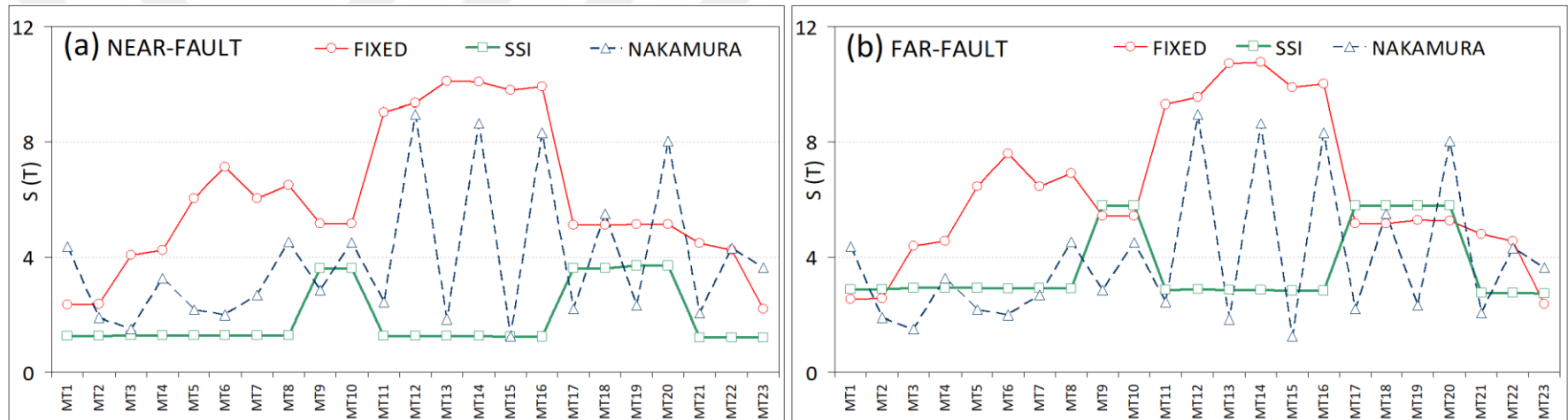


Figure 4.7 Comparisons of spectral amplifications ($S(T)$) of microtremor measurements (Nakamura method) with SSI and fixed under the effects of a) near-fault b) far-fault earthquakes.

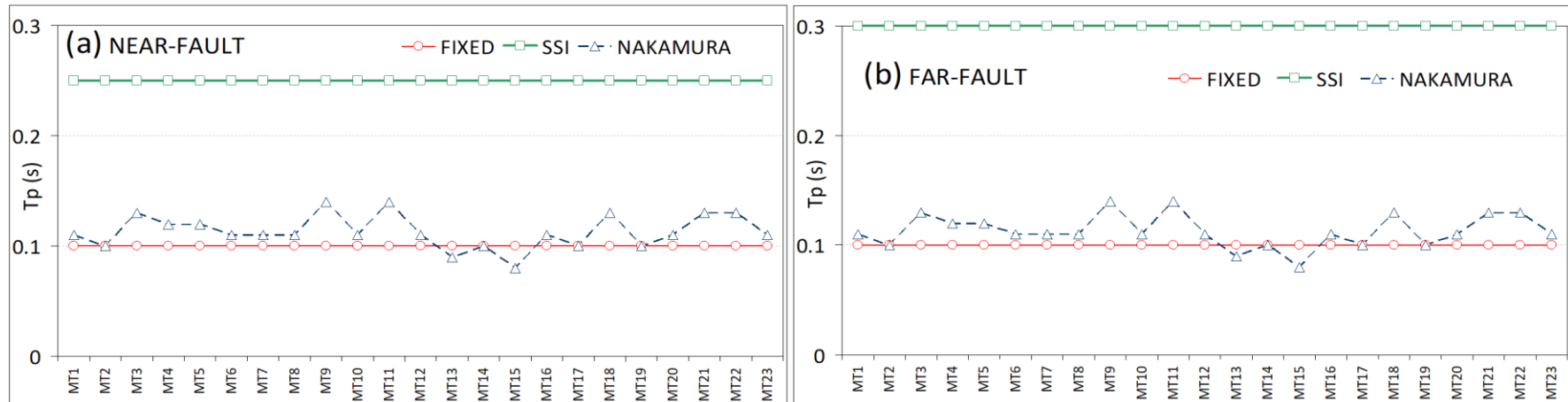


Figure 4.8 Comparisons of predominant periods of microtremor measurements (Nakamura method) with SSI and fixed under the effects of a) near-fault b) far-fault earthquakes.

CHAPTER 5

CONCLUSION

5.1 Conclusion

The dynamic responses (i.e., accelerations, velocities, displacements, natural periods, spectral amplifications) of a historical masonry stone arch bridge through the effort of 3D finite element model (time-history analysis) SSI analysis using under near and far fault earthquakes have been compared to experimentally understand the capability of the modeling by conducting microtremor measurements on the bridge for performance particularly for spectral amplitudes and natural frequencies. Also the spectral responses of HVSR versus HSR(soil) and HSR(base) are compared, according to the data obtained from the microtremor measurement results. The following conclusions could be reached for the investigated historical bridge:

1. It is seen that the near-fault and far-fault motions lead to similar responses of stress distribution as well as maximum stresses in both the fixed and SSI cases. The far-fault earthquake could become a significant effect as much as near-fault earthquake on the bridge responses. In comparison with fixed base solution, it is clearly displayed from the stress distributions that regarding the SSI influences into seismically estimation of bridge response results in larger stress than the ones of fixed base. This clearly indicates that regarding SSI influences for seismically concerns computations of the historical bridge into account could provides a wide of perspective for accurate solutions in safe side. It is clear that the arches (as main part of masonry structural system) under the critical stresses (tensile stresses) could easily address crack regions in a gradual extent and a probable damage under a possible earthquake excitation. If not repaired, the stability and functioning of the bridge will be affected. Thus, the bridge should be protected by performing necessary restoration.

2. The estimations due to HVSR and HSR(base) are more able to produce similar results compared to HSR(soil). However, it should be emphasized that the employed three estimation methodologies do not always guarantee for similarly responding. They may offer the responses in a wide range of scattering. Thus, their results would be more beneficial for spectral contributions when used all together for seismically understanding the bridge behavior. From the microtremor results, it can be generally said that the bridge at majority of locations negatively offers high spectral amplifications ($S(T)$) that exceed the proposed upper limit of design spectrum due to TSC (2007) [140] (i.e., $S(T) > 2.5$). In addition, the predominant periods (T_p) of bridge are obtained in low periods that seem reasonable for low-rise structures like the historical bridge in this study. It can be said that high amplifications could be attributed to the weak or flexible material characteristics, while low amplifications could be due to the good or rigid ones at the corresponding locations of bridge. This could be supported by high amplifications (by Nakamura method) observed at some weak points on the bridge while low amplifications observed at some good points as a preliminary effort. However, determination of the weak or good points at the bridge in detail by microtremors is a separate topic to be investigated in a future study.

3. The experimentally finding of the possibility of resonance case by microtremor is valuable for the bridge. This is in agreement with the finding of resonance case between the bridge and earthquake vibration. Even though the microtremor measurements at the soil and bridge results in the predominant periods in more consistent with the ones of bridge due to fixed base model, it can be said that the spectral responses (resonance case) obtained by microtremor measurements are potentially promising for supporting the conclusions obtained from SSI modeling.

4. The results of the comparisons of spectral accelerations of microtremor measurements the closest values to Nakamura was observed to be the SSI far fault earthquakes. It was found that the effect of far fault earthquakes SSI was significant and the results was similar to the results obtained with 3D model of SSI.

REFERENCES

- [1] Halaçođlu, Y., (1998). *XIV-XVII. Yüzyıllarda Osmanlılarda devlet teşkilatı ve sosyal Yapı*. Türk Tarih Kurumu Yayınları, VII. Dizi, Ankara.
- [2] Şahinalp, M.S., Günal, V., (2012). Spatial analysis of bazaar systems: their location and forms in the Ottoman urbanism culture. *Milli Folklor*, S. **93**, s.149-168.
- [3] General Directorate of Highways (Karayolları Genel Müdürlüğü), (2007). Tarihi köprüler şubesi müdürlüğü, faaliyet raporu. http://www.kgm.gov.tr/SiteCollectionDocuments/KGMdocuments/Duyurular/tarihi_kopruler.pdf, 20 03 2019.
- [4] Sayın, E., (2016). Nonlinear seismic response of a masonry arch bridge. *Earthquakes and Structures*, **10(2)**, 483–494.
- [5] Turer, A., Boz, B., (2008). Computer modeling and seismic performance assessment of historic Aspendos theatre in Antalya, Turkey. *Engineering Structures*, **30(8)**, 2127–2139.
- [6] MCT (Ministry of Culture and Tourism), (2014). Gaziantep Kültür Varlıklarını Koruma Bölge Kurulu Kararı. In Turkish. Kültür ve Turizm Bakanlığı, Gaziantep. <http://www.korumakurullari.gov.tr/Eklenti/44297,gaziantep-ili-oguzeli-ilcesi-yakacik-koyu-koprusunun-te-.pdf>, 12.01.2019.
- [7] Megawati, K., Higashihara, H., Koketsu, K., (2001). Derivation of near-source ground motions of the 1995 Kobe (Hyogoken Nanbu) earthquake from vibration records of the Akashi Kaikyo bridge and its implications. *Engineering Structures*, **23**, pp. 1256–1268
- [8] Pulido, N., Kubo, T, (2004). Near-fault strong motion complexity of the 2000 Tottori earthquake (Japan) from a broadband source asperity model. *Tectonophysics*, **390**, pp.177–192.

- [9] Zhang, S., Wang, G., (2013). Effects of near-fault and far-fault ground motions on nonlinear dynamic response and seismic damage of concrete gravity dams. *Soil Dynamics and Earthquake Engineering*, **53**, 217–29.
- [10] Bray, J.D., Rodriguez-Marek, A., (2004). Characterization of forward-directivity ground motion in the near-fault region. *Soil Dynamics and Earthquake Engineering*, **11**, 815–828
- [11] Brown, A., Saiidi, M.S., (2008). Investigation of near fault vs. far field ground motion effects on a substandard bridge bent. *24th US-Japan bridge engineering workshop*, Minneapolis, Minnesota, session **3**, pp. 111-121.
- [12] Cao, V.V., Ronagh, H.R., (2014). Correlation between seismic parameters of far-fault motions and damage indices of low-rise reinforced concrete frames. *Soil Dynamics and Earthquake Engineering*, **66**, 102-112.
- [13] Kramer, S.L., (1996). *Geotechnical Earthquake Engineering*. Upper Saddle River, NJ: Prentice Hall.
- [14] Chopra, A.K., Chintanapakdee, C., (2001). Comparing response of SDF systems to near-fault and far-fault earthquake motions in the context of spectral regions. *Earthquake Engineering and Structural Dynamics*, **30**, 1769–1789.
- [15] Adanur, S., Altunişik, A.C., Bayraktar, A., Akkose, M., (2012). Comparison of near-fault and far-fault ground motion effects on geometrically nonlinear earthquake behavior of suspension bridges. *Natural Hazards*, **64**, 593–614.
- [16] Soyuluk, K., Karaca, H., (2017). Near-fault and far-fault ground motion effects on cable-supported bridges. *Procedia Engineering*, **199**, 3077–3082.
- [17] Mosleh, A., Razzaghi, M.S., Jara, J., Varum, H., (2016). Seismic fragility analysis of typical pre-1990 bridges due to near-and far-field ground motions. *International Journal of Advanced Structural Engineering*, **8(1)**, 1-9.
- [18] Yazdannejad, K., Yazdani, A., (2018). Bayesian updating of the Park-Ang damage index for RC frame buildings under near-fault ground motions. *Scientia Iranica*, **25(2)**, 606-616.

- [19] Bayraktar, A., Altunişik, A.C., Sevim, B., Kartal, M.E., Türker, T., Bilici, Y., (2009,a). Comparison of near- and far-fault ground motion effect on the nonlinear response of dam–reservoir–foundation systems. *Nonlinear Dynamics*, **58**, 655–673.
- [20] Agrawal, A.K., He, W.L., (2002). A closed-form approximation of near-fault ground motion pulses for flexible structures. *In: 15th ASCE engineering mechanics conference*, New York.
- [21] Wang, G.Q., Zhou, X.Y., Zhang, P.Z., Igel ,H., (2002). Characteristics of amplitude and duration for near fault strong ground motion from the 1999 Chi-Chi, Taiwan earthquake. *Soil Dynamics and Earthquake Engineering*, **22**, 73–96.
- [22] Somerville, P.G., (2003). Magnitude scaling of the near fault rupture directivity pulse. *Physics of The Earth and Planetary Interiors*, **137**, 201–212.
- [23] Akkar, S., Yazgan, U., Gulkan, P., (2005). Drift estimates in frame buildings subjected to near-fault ground motions. *Journal of Structural Engineering Asce*, **131**, 1014–24.
- [24] Mavroeidis G.P., Papageorgiou A.S., (2003). A mathematical representation of near-fault ground motions. *Bulletin of the seismological society of America*, **93**:1099–1131.
- [25] Stewart, J.P., Chou, S., Bray, J.D., Graves, R.W., Somerville, P.G., Abrahamson, N.A., (2001). Ground motion evaluation procedures for performance based design. *Pacific Earthquake Engineering Research Center, Peer Report*, University of California, Berkeley.
- [26] Somerville, P.G., Smith, N.F., Graves, R.W., Abrahamson, N.A., (1997). Modification of empirical strong ground motion attenuation relations to include the amplitude and duration effects of rupture directivity. *Seismological Research Letters*, **68(1)**.
- [27] Liao, W.I., Loh, C.H., Lee, B.H. (2004). Comparison of dynamic response of isolated and non- isolated continuous girder bridges subjected to near-fault ground motions. *Engineering Structures*, **26(14)**, 2173–83.

- [28] Wolf, J.P., Song, C., (2002). Some cornerstones of dynamic soil–structure interaction. *Engineering Structures*, **24**, 13–28.
- [29] Tuladhar, R., Maki, T., Mutsuyoshi, H. .(2008). Cyclic behavior of laterally loaded concrete piles embedded into cohesive soil. *Earthquake Engineering Structural Dynamics*, **37(1)**, 43-59.
- [30] Gazetas, G., Mylonakis, G., (1998). Seismic soil-structure interaction: new evidence and emerging issues. *Geotechnical earthquake engineering and soil dynamics III, American Society of Civil Engineers*, Reston, Virginia, p. 1119-1174.
- [31] Jaber, L., Temsah, Y., Chehade, F.H., Mosallamy, Y.E., (2018). Effect of soil - structure interaction constitutive models on dynamic response of multi-story buildings. *Journal of Engineering Science and Technology Review*, **11(3)**, 56-60.
- [32] Dutta, S.C., Bhattacharya, K., Roy, R., (2004). Response of low-rise buildings under seismic ground excitation incorporating soil–structure interaction. *Soil Dynamics and Earthquake Engineering*, **24**, 893–914.
- [33] Tsai, C.S., Hsueh, C.I., Su, H.C., (2016). Roles of soil-structure interaction and damping in base-isolated structures built on numerous soil layers overlying a half-space. *Earthquake Engineering and Engineering Vibration*, **15(2)**, 387-400.
- [34] Pap, Z., Kollár, L., (2018). Effect of Resonance in Soil-Structure Interaction for Finite Soil Layers. *Periodica Polytechnica Civil Engineering*, **62(3)**, 676-684.
- [35] Tabatabaiefar, S.H.R., Fatahi, B., Samali, B., (2013). Lateral seismic response of building frames considering dynamic soil-structure interaction effects. *Structural Engineering and Mechanics*, **45(3)**, 311-321.
- [36] Güllü, H., Pala, M., (2014). On the resonance effect by dynamic soil–structure interaction: a revelation study. *Natural Hazards*, **72(2)**, 827–847.

- [37] Aoki, T., Sabia, D., Rivella, D., Komiyama, T., (2007). Structural characterization of a stone arch bridge by experimental tests and numerical model updating. *International Journal of Architectural Heritage*, **1**, 227-250.
- [38] Sevim, B., Atamturktur, S., Altunişik, A.C., Bayraktar, A., (2016). Ambient vibration testing and seismic behavior of historical arch bridges under near and far fault ground motions. *Bulletin of Earthquake Engineering*, **14**, 241–259.
- [39] Hadianfard, M.A., Rabiee, R., Sarshad, A., (2017). Assessment of vulnerability and dynamic characteristics of a historical building using microtremor measurements. *International Journal of Civil Engineering*, **15**, 175–183.
- [40] Herak, M., (2011). Overview of recent ambient noise measurements in Croatia in free-field and in buildings. *Geofizika*, **28**, 21–40.
- [41] Molnar, S., Cassidy, J. F., Castellaro, S., Cornou, C., Crow, H., Hunter, J.A., Yong, A., (2018). Application of microtremor horizontal-to-vertical spectral ratio (MHVSR) analysis for site characterization: State of the art. *Surveys in Geophysics*, **39(4)**, 613-631.
- [42] Chatelain, J.L., Guillier, B., Cara, F., Duval, A.M., Atakan, K., Bard, P.Y., The WP02 SESAME Team, (2008). Evaluation of the experimental conditions on H/V results from ambient noise recordings. *Bulletin of Earthquake Engineering*, **6**, 33-74.
- [43] Özdağ, C., Gönenç, T., Akgün, M., (2015). Dynamic amplification factor concept of soil layers: a case study in İzmir (Western Anatolia). *Arabian Journal of Geosciences*, **8(11)**, 10093–10104.
- [44] Pamuk, E., Özdağ, Ö.C., Özyalın, Ş., Akgün, M., (2017). Soil characterization of Tınaztepe region (İzmir/Turkey) using surface wave methods and Nakamura (HVSR) technique. *Earthquake Engineering and Engineering Vibration*, **16(2)**, 447-458.
- [45] Gosar, A., (2012). Determination of masonry building fundamental frequencies in five Slovenian towns by microtremor excitation and implications for seismic risk assessment. *Natural Hazards*, **62(3)**, 1059-1079.

- [46] Ünay, A.İ., (1997). A method for the evaluation of the ultimate safety of historical masonry structures. *Ph.D. Dissertation*, METU, Ankara.
- [47] Baykasoğlu, A., Güllü, H., Çanakçı, H., Özbakır, L., (2008). Prediction of compressive and tensile strength of limestone. *Expert Systems with Applications*, **35**, 111-128.
- [48] Veletsos, A.S., Prasad, A. (1989). Seismic interaction of structures and soils: stochastic approach. *Journal of Structural Engineering ASCE*, **115**, 935–956.
- [49] Aviles, J., Perez-Rocha, L.E. (1998). Site effects and soil-structure interaction in the Valley of Mexico. *Soil Dynamics and Earthquake Engineering*, **17**, 29-39.
- [50] Stewart, J.P., Fenres, G.L., Seed, R.B. (1999). Seismic soil–structure interaction in buildings I: analytical method. *Journal of Geotechnical and Geoenvironmental Engineering*, **125(1)**, 26–37.
- [51] Mylonakis, G., Gazetas, G., (2000). Seismic soil–structure interaction: beneficial or detrimental? *Journal of Earthquake Engineering*, **4(3)**, 277–301
- [52] Park, S.W., Ghasemi, H., Shen, J., Somerville, P.G., Yen, W.P., Yashinsky, M., (2004). Simulation of the seismic performance of the Bolu Viaduct subjected to near-fault ground motions. *Earthquake Engineering & Structural Dynamics*, **33**, 1249-1270.
- [53] Marek, A.R., Bray, J.D., (2006). Site effects for near-fault forward-directivity motions. *Journal of Geotechnical and Geoenvironmental Engineering*, **132**, 1611-1620.
- [54] Jalali, R.S., Jokandan, M.S., Trifunac, M.D., (2012). Earthquake response of a three-span simply supported bridge to near-field pulse and permanent displacement step. *Soil Dynamics and Earthquake Engineering*, **43**, 380-397.
- [55] Davoodi, M., Jafari, M.K., Hadiani, N., (2013). Seismic response of embankment dams under near-fault and far-field ground motion excitation. *Engineering Geology*, **158**, 66-76.

- [56] Tongaonkar, N.P., Jangid, R.S., (2003). Seismic response of isolated bridges with soil–structure interaction. *Soil Dynamics and Earthquake Engineering*, **23(4)**, 287–302.
- [57] Quanani, M., Tiliouine, B., (2015). Effects of foundation soil stiffness on the 3-D modal characteristics and seismic response of a highway bridge. *KSCE Journal of Civil Engineering*, **19(4)**, 1009–1023.
- [58] Güllü, H., Karabekmez, M., (2017). Effect of near fault and far fault earthquakes on a historical masonry mosque through 3D dynamic soil-structure interaction. *Engineering Structures*, **152**, 465–492.
- [59] Akkar, S., Moghimi, S., Arıcı, Y., (2018). A study on major seismological and fault-site parameters affecting near-fault directivity ground-motion demands for strike-slip faulting for their possible inclusion in seismic design codes. *Soil Dynamics and Earthquake Engineering*, **104**, 88-105.
- [60] Bielak, J., (1976). Modal analysis for building-soil interaction. *Journal of the Engineering Mechanics Division ASCE*, **102**, 771-786.
- [61] Luco, J.E., Trifunac, M.D., Wong H.L., (1987). On the apparent change in dynamic behavior of a nine-story reinforced concrete building. *Bulletin of the Seismological Society of America*, **77**, 1961-1983.
- [62] Burman, A., Nayak, P., Agrawal, P., Maity, D., (2012). Coupled gravity dam–foundation analysis using a simplified direct method of soil–structure interaction. *Soil Dynamics and Earthquake Engineering*, **34**, 62–68.
- [63] Cakir, T., (2013). Evaluation of the effect of earthquake frequency content on seismic behavior of cantilever retaining wall including soil–structure interaction. *Soil Dynamics and Earthquake Engineering*, **45**, 96-111.
- [64] Bendat, J., Piersol, A., (1986). *Random data: analysis and measurement procedures. 2nd edition*, Wiley, New York.
- [65] Caetano, E., (2000). Dynamic of cable-stayed bridges: experimental assessment of cable-structure interaction. *PhD Thesis, Engineering Faculty of University of Porto, Portugal*.

- [66] Ramos, J.L.F.S., (2007). Damage identification on masonry structures based on vibration signatures. *PhD Thesis. University of Minho, Portugal.*
- [67] Bayraktar, A., Türker, T., Sevim, B., Altunişik, A.C., Yildirim, F., (2009). Modal parameter identification of Hagia Sophia bell-tower via ambient vibration test. *Journal of Nondestructive Evaluation*, **28**, 37–47.
- [68] Sevim, B., Bayraktar, A., Altunişik, A.C., Atamturktur, S., Birinci, F., (2011). Assessment of nonlinear seismic performance of a restored historical arch bridge using ambient vibrations. *Nonlinear Dynamics*, **63(4)**, 755–770.
- [69] Calcina, S.V., Piroddi, L., Ranieri, G., (2016). Vibration analysis of historic bell towers by means of contact and remote sensing measurements. *Nondestructive Testing and Evaluation*, **31**, 331-359.
- [70] Altunişik, A.C., Adanur, S., Genc, A.F., Gunaydın, M., Okur, F.Y., (2016). An Investigation of the Seismic Behaviour of an Ancient Masonry Bastion Using Non-Destructive and Numerical Methods. *Experimental Mechanics*, **57**, 245–259.
- [71] Nakamura, Y., (1989). A method for dynamic characteristics estimations of subsurface using microtremors on the ground subsurface. *Quarterly Report of Railway Technical Research Institute, Japan*, **30(1)**, 25-33.
- [72] Gallipoli, M.R., Mucciarelli, M., Castro, R.R., Monachesi, G., Contri, P., (2004). Structure, soil-structure response and effects of damage based on observations of horizontal-to-vertical spectral ratios of microtremors. *Soil Dynamics and Earthquake Engineering*, **24**, 487, 495.
- [73] Gosar, A., Roser, J., Sket-Motnikar, B., Zupancic, P., (2010). Microtremor study of site effects and soil-structure resonance in the city of Ljubljana (central Slovenia). *Bulletin of Earthquake Engineering*, **8**, 571–592.
- [74] Gentile C., Saisi A., (2007). Ambient vibration testing of historic masonry towers for structural identification and damage assessment. *Construction and Building Materials*, **21**, 1311-1321.

- [75] Aras F., Kretevska L., Altay G., Tashkov L., (2011). Experimental and numerical modal analysis of a historical masonry place. *Construction and Building Materials*, **25(1)**, 81-91.
- [76] Atamturktur, S., Bornn, L., Hemez, F., (2011). Vibratioan characteristics of vaulted masonry monuments undergoing differantial support settlement. *Engineering Structures*, **33**, 2472-2484.
- [77] Wolf, J.P., (1985). Dynamic soil structure interaction. Englewood Cliffs (N.J.): Prentice-Hall.
- [78] Proske, D., Gelder, P., (2009). *Safety of historical stone arch bridges*. Springer-Verlag, Heidelberg Dordrecht, London, U.K.
- [79] Asteris, P.G., Tzamtzis, A.D., (2003). Nonlinear seismic response analysis of realistic gravity dam reservoir systems. *International Journal of Nonlinear Sciences and Numerical Simulation*, **4(4)**, 329–338.
- [80] Manos, G.C., Soulis, V.J., Diagouma, A., (2008). Numerical investigation of the behaviour of the church of Agia Triada, Drakotrypa, Greece. *Advances in Engineering Software*, **39**, 284-300.
- [81] Asteris, P.G., Chronopoulos, M.P., Chrysostomou, C.Z., Varum, H., Plevris, V., Kyriakides, N., Silva, V., (2014). Seismic vulnerability assessment of historical masonry structural systems. *Engineering Structures*, **62–63**, 118-134.
- [82] Lourenco, P.B., (1996). Computational strategies for masonry structures. *Doctoral dissertation*, TU Delft, Delft University of Technology.
- [83] Emre, Ö., Duman, T.Y., Olgun, Ş., Elmacı, H., Özalp, S., (2018). Active fault map of Turkey. General Directorate of Mineral Research and Exploration, Ankara, Turkey, http://www.mta.gov.tr/v3.0/sayfalar/hizmetler/doc/yenilenmis_diri_fay_harit_alari/gaziantep.pdf, 13.12.2018.
- [84] Güllü, H., Ansal, M.A., Özbay, A., (2008). Seismic hazard studies for Gaziantep city in South Anatolia of Turkey. *Natural Hazards*, **44(1)**, 19-50.

- [85] AFAD (T.R. Ministry of Interior-President of Disaster and Emergency Management), (2018). Earthquake Hazard Map of Turkey. <https://www.afad.gov.tr/tr/24212/Turkiye-Deprem-Tehlike-Haritasi>, 24.03.2019.
- [86] AFAD (T.R. Ministry of Interior-President of Disaster and Emergency Management), (2019). http://kyhdata.deprem.gov.tr/2K/kyhdata_v4.php?dst=TU9EVUxFX05BTUU9c3RhGlvbnMmTU9EVUxFX1RBU0s9c2hvdvZNT0RVTEVfU1VCVEFTSz1ieVN0YUIEJk1PRFVMRV9UQVJHRVQ9NDYxNiZUQVJHRVRfTEFUTE9OPTM3LjM3NTQ3LDM2LjgzODM2, 02.03.2019.
- [87] Li, M., Lu, X., Lu, X., Ye, L., (2014). Influence of soil-structure interaction on seismic collapse resistance of super-tall buildings. *Journal of Rock Mechanics and Geotechnical Engineering*, **6**, 477-485.
- [88] Pitilakis, D., Clouteau, D., (2010). Equivalent linear substructure approximation of soil foundation-structure interaction: model presentation and validation. *Bulletin of Earthquake Engineering*, **8(2)**, 257-282.
- [89] Preisig, M., Jeremic, B., (2005). Nonlinear finite element analysis of dynamic soil-foundation-structure interaction. *SFSI report, NSF-CMS-0337811, Department of Civil and Environmental engineering*. University of California, Davis.
- [90] Livaoglu, R., Dogangun, A., (2007). Effect of foundation embedment on seismic behavior of elevated tanks considering fluid–structure-soil interaction. *Soil Dynamics and Earthquake Engineering*, **27**, 855-863.
- [91] Tabatabaiefar, H.R., Massumi, A., (2010). A simplified method to determine seismic responses of reinforced concrete moment resisting building frames under influence of soil–structure interaction. *Soil Dynamics and Earthquake Engineering*, **30**, 1259-1267.
- [92] Güllü, H., Jaf, H.S., (2016). Full 3 d nonlinear time history analysis of dynamic soil-structure interaction for a historical masonry arch bridge. *Environmental Earth Sciences*, **75(21)**, 1421.

- [93] Ziekiewicz, O.C., Taylor, R.L., (1989). *The Finite Element Method*, McGraw-Hill, London.
- [94] Wilson, H.H., Krummenacher, R., (1957). Geology and oil prospects of Gaziantep region, SE, Turkey. *Petrol Daire Başkanlığı teknik arşivi*, Ankara (unpublished).
- [95] Nadjai, A., Johnson, D., (1996). Elastic analysis of spatial shear wall systems with flexible bases. *The Structural Design of Tall Buildings*, **5(1)**, 55-72.
- [96] Rashed, Y.F., (2005). A Boundary domain element method for analysis of building raft foundations. *Engineering Analysis with Boundary Elements*, **29(9)**, 859-877.
- [97] Chowdhury, I., Singh, J.P., Tilak, R., (2012). Seismic response of well foundation with dynamic soil structure interaction. *In Proceedings 15th World Conference in Earthquake Engineering*. Lisbon, Portugal.
- [98] SAP2000 (v.20), (2019). Integrated finite element analysis and design of structures basic analysis reference manual. Computer and Structures Inc., California, Berkeley, <https://www.csiamerica.com/products/sap2000>, 15.01.2019.
- [99] Tavakoli, H.R., Naeef, M., Salari, A., (2011). Response of RC structures subjected to near-fault and far-fault earthquake motions considering soil-structure interaction. *International Journal of Civil and Structural Engineering*, **1(4)**, 881-896.
- [100] Gönen, H., Dogan, M., Karacasu, M., Özbaşaran, H., Gokdemir, H., (2013). Structural failures in retrofit historical masonry arch bridge. *Engineering Failure Analysis*, **35**, 334-342.
- [101] Cappellini, A., Cigada, A., Vanali, M., Leva, D., Rivolta, C., (2014). Advantages and drawbacks in the use of non-contact radar techniques to perform dynamic measurements. *Journal of Civil Structural Health Monitoring*, **4**, 303–311.

- [102] Livaoglu, R., Basturk, M.H., Dogangün, A., Serhatoglu, C., (2016). Effect of geometric properties on dynamic behavior of historic masonry minaret. *KSCE Journal of Civil Engineering*, **20**, 2392-2402.
- [103] Jaiswal, R.K., Mishra S., (2008). Seismic instrumentation: Indian perspective. *7th International Conference and Exposition on Petroleum Geophysics* Hyderabad, India, pp.385-390.
- [104] SESAME, (2004). Guidelines for the implementation of the H/V spectral ratio technique on ambient vibrations: measurements, processing and interpretation SESAME European Research Project WP12-Deliverable D23.12. [ftp://ftp.geo.uib.no/pub/seismo/SOFTWARE/SESAME/USER GUIDELINES/SESAME-HV-User-Guidelines.pdf](ftp://ftp.geo.uib.no/pub/seismo/SOFTWARE/SESAME/USER_GUIDELINES/SESAME-HV-User-Guidelines.pdf)mistr, 01.03.2019
- [105] Geopsy, (2019). Geopsy software (Geophysical Signal Database for Noise Array Processing). <http://www.geopsy.org/download.php>, 23.03.2019.
- [106] GeoBox., (2019). SR04 GeoBox-SARA Electronic Instruments. http://www.sara.pg.it/documents/commercial/SR04_GEOBOX_DATASHEET_ENG.pdf, 17.03.2019.
- [107] Konno, K., Ohmachi, T., (1998). Ground motion characteristics estimated from spectral ratio between horizontal and vertical components. *Bulletin of the Seismological Society of America*, **88**, 1, 228-241.
- [108] Mucciarelli, M., Monachesi, G., (1998). A quick survey of local amplifications and their correlation with damage observed during the Umbro-Marchesan (Italy) earthquake of September 26, 1997. *Journal of Earthquake Engineering*, **2**, 1-13.
- [109] Mucciarelli, M., Monachesi, G., (1999). The Bovec (Slovenia) earthquake, April 1998: a preliminary correlation among damage, ground motion amplification and building frequencies. *Journal of Earthquake Engineering*, **3**, 317-327.
- [110] General Directorate of Highways (Karayolları Genel Müdürlüğü), (2013). Tarihi Yakacık Köyü Köprüsü Restorasyon Analizi. 5th Regional Directorate of Highways, Mersin.

- [111] Gucci, N., Barsotti, R., (1995). A non-destructive technique for the determination of mortar load capacity in situ. *Materials and Structures*, **28**, pp.276–283.
- [112] Hees, R.P.J., Binda, L., Papayianni, I., Toumbakari, E., (2004). Characterization and damage analysis of old mortars. *Materials and Structures*, **37**, pp.644–648.
- [113] Böke, H., Akkurt, S., İpekoğlu, B., Uğurlu, E., (2006). Characteristics of brick used as aggregate in historic brick-lime mortars and plasters. *Cement and Concrete Research*, **36(6)**, pp.1115–1122.
- [114] Domède, N., Pons, G., Sellier, A., Fritih, Y., (2008) Mechanical behaviour of ancient masonry. *Materials and Structures*, **42**, 123-133.
- [115] Giamundo, V., Sarhosis, V., Lignola, G.P., Sheng, Y., Manfredi, G., (2014). Evaluation of different computational modelling strategies for the analysis of low strength masonry structures. *Engineering Structures*, **73**, 160-169.
- [116] Sarhosis, V., Sheng, Y., (2014). Identification of material parameters for low bond strength masonry. *Engineering Structures*, **60**, 100-110.
- [117] Sarhosis, V., Oliveira, D.V., Lemos, J.V., Lourenco, P.B., (2014). The effect of skew angle on the mechanical behaviour of masonry arches. *Mechanics Research Communications*, **61**, 53–59.
- [118] Mann, W., (1983). Compressive strength of masonry statistical evaluation of experiments with power functions. *Mauerwerk-Kalender*, pp.687–699.
- [119] Schubert, P., Hoffmann, G., (1994). Compressive strength of mortar in masonry significance, influences, test methods, requirements. *Proceedings of the 10th International Brick and Block Masonry Conference*, Calgary, Alberta, 1335-1344.
- [120] Latka, D., Serega, S., Matysek, P., (2018). Estimation of mortar compressive strength based on specimens extracted from masonry bed joints. *11th International conference on structural analysis of historical construction: an interdisciplinary approach*, Cusco, Peru, **18**, 577-586.

- [121] EN 1996-1-1. Eurocode 6-Design of masonry structures-Part 1-1: General rules for reinforced and unreinforced masonry structures. European Committee For Standardization, Brussels, November, 2015.<https://www.phd.eng.br/wp-content/uploads/2015/02/en.1996.1.1.2005.pdf>, 07.03.2019.
- [122] Ril 805, (1999). Richtlinie 805: *Tragsicherheit bestehender Eisenbahnbrücken*, DB Netz AG 2002.
- [123] Karaton, M., Aksoy, H.S., Sayın, E., Calayır, Y., (2017). Nonlinear seismic performance of a 12th century historical masonry bridge under different earthquake levels. *Engineering Failure Analysis*, **79**, 408–421.
- [124] Karaton, M., Aksoy, H.S., (2018). Seismic damage assessment of an 891 years old historic masonry mosque. *Periodica Polytechnica Civil Engineering*, **62**, 10.3311/PPci.10270.
- [125] Papayianni, I., Stefanidou, M., (2003). Mortars for intervention in monuments and historical buildings. *Structural Studies, Repairs and Maintenance of Heritage Architecture*, VIII, CA Brebbia (Ed), WIT-Press, Southampton, pp.57–64.
- [126] DIN 1053-100., (2004). *Mauerwerk: Berechnung auf der Grundlage des semiprobabilistischen Sicherheitskonzeptes*. NABau im DIN/Beuth Verlag: Berlin, 7/2004.
- [127] Özsavcı, L., (2017). Kevser Mühendislik Sondaj & Zemin Araştırma San. Tic. Ltd. Şti. Gaziantep, Turkey.
- [128] Ramos, L.F., Lourenço, P.B., (2004). Modeling and vulnerability of historical city centers in seismic areas: a case study in Lisbon. *Engineering Structures*, **26(9)**, 1295–1310.
- [129] Anbazhagan, P., Sheikh, M.N., Parihar, A., (2013). Influence of rock depth on seismic site classification for shallow bedrock regions. *Natural Hazards Review*, **14(2)**, 108-121.

- [130] MTA (Turkish General Directorate of Mineral Research and Exploration), (2018). <http://www.mta.gov.tr/v3.0/sayfalar/hizmetler/doc/HATAY.pdf>, 14.04.2018.
- [131] Power, M.S., Chang, C.Y., Idriss, I.M., (1986). Variation of earthquake ground motion with depth. *Proceedings of the Third US. National Conference on Earthquake Engineering*, Charleston, South Carolina, August.
- [132] Borchardt, R.D., Wenworth, C.M., Janssen, A., Fumal, T., Gibbs, J., (1991). Methodology for predictive gis mapping of special study zones for strong ground shaking in the San Francisco bay region. *Proc. 4th Inter. Conf. On Seismic Zonation*, Stanford, California, pp.545-552.
- [133] Finn, W.D.L., (1991). Geotechnical engineering aspects of microzonation. *Proc. of the Fourth International Conference on Seismic Zonation, August 25th-29th*, Stanford, California.
- [134] Ansal, A.M., Lav, A.M., İyisan, R., Erken, A., (1994). Effect of geotechnical factors in march 13, 1992 Erzincan earthquake, performance of ground and soil structure during earthquakes. *13 th Int. Conf. Soil Mechanics and Foundation Engineering.*, New Delhi, 49-54.
- [135] Anderson, J.G., Lee, Y., Zeng, Y., Day, S.M., (1996). Control of strong motion by upper 30 meters. *Bulletin of the Seismological Society of America*, **86**, pp.1749-1759.
- [136] Fatahi, B., Far, H., Samali, B., (2014). Soil-structure interaction vs site effect for seismic design of tall buildings on soft soil. *Geomechanics and Engineering*, **6**, 293-320.
- [137] Ates, S., Constantinou, M.C., (2011). Example of application of response spectrum analysis for seismically isolated curved bridges including soil-foundation effects. *Soil Dynamics and Earthquake Engineering*, **31**, 648–661.
- [138] Torabi, H., Rayhani, M.T., (2014). Three dimensional finite element modeling of seismic soil–structure interaction in soft soil. *Computers and Geotechnics*, **60**, 9–19.

- [139] Ghandil, M., Behnamfar, F., (2017). Ductility demands of MRF structures on soft soils considering soil-structure interaction. *Soil Dynamics and Earthquake Engineering*, **92**, 203-214.
- [140] TSC (Turkish Seismic Code), (2007). Specification for structures to be built in disaster areas. In Turkish: Deprem Bölgelerinde Yapılacak Binalar Hakkında Yönetmelik; <http://www.koeri.boun.edu.tr/deprenmuh/eski/DBYBHY-2007-KOERI.pdf>, 23.03.2017.
- [141] Zangeneh, A., Svedholm, C., Andersson, A., Pacoste, C., Karoumi, R., (2018). Identification of soil-structure interaction effect in a portal frame railway bridge through full-scale dynamic testing. *Engineering Structures*, **159**, 299-309.
- [142] Bhaumik, L., Raychowdhury, P., (2013). Seismic response analysis of a nuclear reactor structure considering nonlinear soil-structure interaction. *Nuclear Engineering and Design*, **265**, 1078-1090.
- [143] Marzban S, Banazadeh M, Azarbakht A., (2011). Seismic performance of concrete shear wall frames considering soil foundation-structure interaction. *Proceedings of the 8th International Conference on Structural Dynamics (EURODYN 2011)*, Leuven, Belgium, 4-6 July, G. De Roeck, G. Degrande, G. Lombaert, G. Muller (Eds.), ISBN: 978-90-760-1931-4.
- [144] Marzban, S., Banazadeh, M., Azarbakht, A., (2014). Seismic performance of reinforced concrete shear wall frames considering soil–foundation–structure interaction. *The Structural Design of Tall and Special Buildings*, **23(4)**, 302-318.
- [145] Casolo, S., Diana, V., Uva, G., (2017). Influence of soil deformability on the seismic response of a masonry tower. *Bulletin of Earthquake Engineering*, **15**, 1991–2014.
- [146] Koseoglu, G.C., Canbay, E., (2015). Assessment and rehabilitation of the damaged historic Cenabı Ahmet Pasha Mosque. *Engineering Failure Analysis*, **57**, 389-398.

- [147] Kvalseth, T.O., (1985). Cautionary note about R^2 . *The American Statistician*, **39**, 279–285.
- [148] Güllü, H., (2012). Prediction of peak ground acceleration by genetic expression programming and regression: a comparison using likelihood-based measure. *Engineering Geology*, **141-142**, 92-113.
- [149] Güllü, H., Canakci, H., Alhashemy, A., (2018). A ranking distance analysis for performance assessment of UCS Versus SPT-N correlations. *Arabian Journal for Science and Engineering*, 1-13.



CURRICULUM VITAE

PERSONAL INFORMATION

Surname, Name: ÖZEL, Feyzullah

Nationality: Turkish (Republic of Turkey)

Date and Place of Birth: 23 July 1971, Andırın / Kahramanmaraş

Phone: +90 538 715 6880

Email: fozel23@hotmail.com

EDUCATION

Degree	Institution	Year of Graduation
MS	Gaziantep University	2019
BS	Gaziantep University	1994

WORK EXPERIENCE

Year	Place	Enrollment
2001-Present	General Directorate of Highways	Costruction Control Chief
1994-2001	STFA, Yüksel, Gürbağ Construction Companies	Site Engineer, Site Chief